

# Toward An Adhesion Based Measurement of Strain-Dependent Surface Stress in Soft Solids

by  
Jeremy K. Thaller

Professor Katharine E. Jensen, Advisor



A thesis submitted in partial fulfillment  
of the requirements for the  
Degree of Bachelor of Arts with Honors  
in Physics

WILLIAMS COLLEGE  
Williamstown, Massachusetts  
April 26, 2019

# Abstract

Surface stress, or surface tension, is a fundamental material property of interfaces. However, our understanding of solid surface tension and how it changes with deformation remains limited because it is difficult to measure in traditional stiff materials. Soft materials, including gels, provide a unique opportunity to measure these fundamental properties because they can be stretched elastically to very large strains. In this thesis, we have developed a new, adhesion-based approach to measure the solid surface stress of compliant materials as a function of applied strain. This approach is applicable to a wide range of soft materials.

Return to this continually....

# Executive Summary

This thesis describes a new method for measuring strain dependent surface stress in soft solids, as well as the corresponding measurements for two silicone polymer gels. Over the past several years, recent attempts to measure surface stress in gels have returned a cornucopia of conflicting results, differing significantly in similar materials. Recently, Xu, Jensen et al. suggested that this discrepancy is an artifact of the strain state of the gels, and made the first measurement of strain-dependent surface stress,  $\Upsilon(\epsilon)$ , in solids [1]. In this paper, the authors reported that the surface stress changed dramatically under applied strain. At 18% strain, the surface stress more than doubled.



Figure 1: This is first direct measurement of strain dependent surface stress in solids [1]. Using a compliant silicone gel, surface stress,  $\Upsilon$ , was found to grow linearly as a function of strain,  $\epsilon$ .

Over the past year, we have helped develop a new method for measuring  $\Upsilon(\epsilon)$  in soft solids. Our adhesion-based technique can be applied to a wide variety of stretchable materials. Additionally, we have build our own equibiaxial stretching apparatus, improving upon the earlier published design [1] to produce nearly twice the strain in identical materials. Using this technique we have measured the adhesion energy and surface stress in two types of silicone, as well as preliminary  $\Upsilon(\epsilon)$  measurements as we work towards recreate the controversial 2017 measurement.

Our results suggest that the surface tension in gels does significantly change under strain. The figure below is an example of how you can visually see this change for a single silica sphere sitting in a silicone substrate. As the underlying gel is stretched, the surface tension increases, reducing the depth into which the sphere sits.

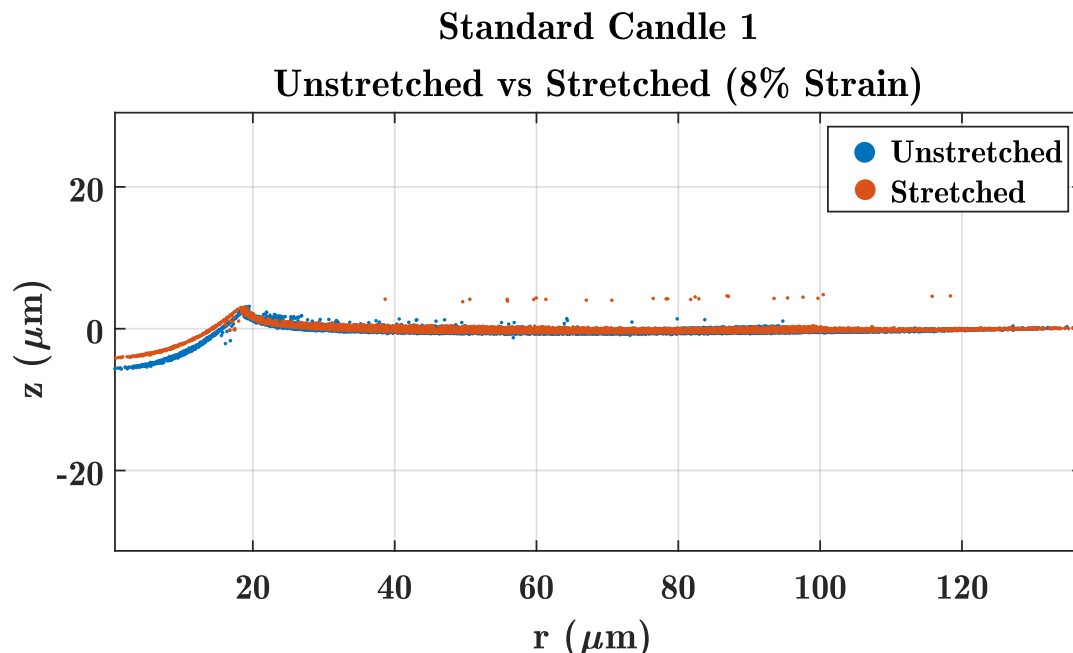


Figure 2: The side profile of the same silica sphere sitting in a silicone substrate before and after stretch. When a strain is applied, the sphere's indentation into the substrate is shallower. Substrate is Gelest PDMS with stiffness  $E = 6.3 \text{ kPa}$ .

I will continue to update this section. I hope to have a much more compelling graph to share, one more similar to Figure 1.

# Acknowledgements

Make sure to include: KEJ, Mr. Josh Kang aka super soldier, Abdullah, Michael Taylor and Jason Mativi, Professor Strait for teaching me everything I know about Vibrations, Waves, and Optics. Professor Majumbles. Probably my track coaches. Parents I guess.

# Contents

<b>Abstract</b>	i
<b>Executive Summary</b>	ii
<b>Acknowledgements</b>	iv
<b>1 Introduction</b>	1
1.1 Motivations . . . . .	1
1.2 Historical Context . . . . .	1
1.2.1 Development of Surface Tension . . . . .	1
1.2.2 Surface Tension in Solids . . . . .	2
1.2.3 Surface Stress Effects in Soft Solids . . . . .	3
1.2.4 Direct Measurement of Solid Surface Stresses . . . . .	4
1.3 Outline of the Thesis . . . . .	6
<b>2 Experimental Approach: Setup, Data Acquisition, &amp; Analysis</b>	7
2.1 Measuring Surface Stress via Adhesion . . . . .	7
2.1.1 Beyond Hertzian Mechanics and JKR Theory . . . . .	7
2.1.2 Force Balance Derivation . . . . .	8
2.1.3 Experimental Approach . . . . .	10
2.2 Preparing a Substrate . . . . .	11
2.3 Stretching Apparatus . . . . .	11
2.3.1 Stretcher Design . . . . .	12
2.4 Calibration . . . . .	13
2.4.1 Measuring Strain . . . . .	14
2.5 Material Characterization . . . . .	16
2.5.1 Hertzian Contact Mechanics Derivation? . . . . .	17
2.6 Putting it all Together . . . . .	18
<b>3 Data Acquisition and Image Analysis</b>	19
3.1 Fluorescent Confocal Microscopy . . . . .	19
3.2 Applying Fluorescent Confocal Microscopy to our Sample . . . . .	21
3.2.1 Raw Data Files . . . . .	22

<i>CONTENTS</i>	vi
3.3 Image Analysis . . . . .	23
3.3.1 Particle Location . . . . .	24
3.3.2 Depth and Radius Determination . . . . .	24
<b>4 Surface Stress and Adhesion Results</b>	<b>32</b>
4.1 Organosilicon Polymer Chemistry . . . . .	32
4.2 Preliminary Data: Gelest . . . . .	35
4.2.1 Standard Candles . . . . .	35
4.3 Dow-Corning PDMS . . . . .	35
<b>5 Future Work</b>	<b>39</b>
5.1 Neue Materialen: Gummibärli . . . . .	39
<b>A Stretching Apparatus Design</b>	<b>40</b>
A.1 Details of Stretcher Design . . . . .	40
<b>B Fluorescent Bead Recipe</b>	<b>43</b>
B.1 Preparing a Fluorescent Bead Solution . . . . .	43
<b>C MATLAB Code</b>	<b>44</b>
C.0.1 Confocal Analysis Codes . . . . .	44
C.0.2 Strain Calculation Codes . . . . .	45
C.0.3 Silicone Characterization Measurements . . . . .	45

# List of Figures

1	Surface Stress vs. Strain in Silicone . . . . .	ii
2	Side Collapse Comparison . . . . .	iii
1.1	Three-Phase Diagram . . . . .	4
2.1	Spherical Cap Geometry . . . . .	9
2.2	Prepared Substrate Profile . . . . .	12
2.3	Stretching Apparatus Design . . . . .	13
2.4	Side Profile of Stretching Apparatus . . . . .	14
2.5	Bright-field pre and post image processing . . . . .	15
2.6	Unstretched . . . . .	16
2.7	Stretched . . . . .	16
2.8	Bulk Modulus Test . . . . .	17
3.1	Minsky Patent Diagram . . . . .	19
3.2	Fluorescent Confocal Microscopy . . . . .	20
3.3	Nikon Ti2 Microscope Base . . . . .	21
3.4	The surface plane of a silica bead in silicone . . . . .	22
3.5	Vertical path through image stack . . . . .	23
3.6	Particle Located: Normalized-Axes . . . . .	24
3.7	Particle Located: Stretched-Axes . . . . .	25
3.8	Particle Located: Top View . . . . .	26
3.9	Collapsed Side Profile . . . . .	27
3.10	Collapsed Side Profile: Zoomed . . . . .	28
3.11	Circle Fit . . . . .	29
3.12	Circle Fit Zoomed . . . . .	30
3.13	D vs R plot . . . . .	31
4.1	DMS-V31 . . . . .	32
4.2	HMS-301 . . . . .	33
4.3	Side Collapse Comparison . . . . .	36
4.4	Glass vs. Stretched d vs. R . . . . .	37
4.5	Gelest W-Y Fit . . . . .	37

*LIST OF FIGURES*

viii

4.6 D-C W $\Upsilon$ Fit . . . . .	38
A.1 Stretching Apparatus Design Document . . . . .	41
A.2 Stretcher outer-ring . . . . .	42

# Chapter 1

## Introduction

### 1.1 Motivations

Soft Condensed Matter Physics includes the study of colloids, liquid crystals, polymers, complex fluids, rubbers, foams, many biological materials, and - what we devote most of our time to studying in the Jensen lab - gels. From cosmetics to sticky notes, soft solids are ubiquitous in everyday life and are of growing interest due to their unique properties compared to traditional (hard) engineering materials. It is important to understand how such ubiquitous materials behave, especially when put under the strains of life. Accordingly, there

### 1.2 Historical Context

#### 1.2.1 Development of Surface Tension

Though few people may know the term, surface stress is a familiar concept in everyday phenomena: water droplets bead up into spheres, paperclips can float on water despite being made of dense iron, and water striders navigate the water's surface thanks to their hydrophobic legs. Each of these marvels is a result of **surface stress**,  $\gamma$ , the energetic cost per unit area to create new surface [2]. The water strider, for example, exerts a force on the water due to gravity. Because creating new surface costs energy, the water resists deformation, providing a restorative force that effectively balances the insect's weight to keep it afloat. Likewise, water droplets bead up and liquid surfaces are smooth because  $\gamma$  opposes surface stretching, acting to minimize the surface-to-volume ratio of the liquid [3, 4]

Consider returning here and adding after reading de Gennes

The energy associated with particles in the bulk is less than that of the particles at the surface. Molecules beneath the surface are attracted by the particles around them in every

direction. In contrast, the particles at the surface are only attracted by the molecules directly adjacent to them. As a result of these less favorable interactions, they are in a state of higher energy compared to molecules in the bulk. The difference in energy between particles in the bulk compared to the surface is known as the **surface free energy**,  $\gamma$ , often written as just surface energy. Equivalently,  $\gamma$  can also be defined as the reversible work per unit area to create new surface by cutting. This exposes new particles to the surface. When the surface of a fluid is stretched, however, new atoms or molecules arrive at the surface, maintaining the number of atoms per unit area as a constant value. Therefore, the surface energy is the same as the surface stress for a fluid and equal to a constant value. Because of this,  $\gamma$  and  $\Upsilon$  have are often referred to interchangeably as **surface tension**. While conceptually the energetics are similar in solid materials, the situation becomes more complicated for materials that cant flow.

### 1.2.2 Surface Tension in Solids

Move to later discussion of molecular origins

In metals, the origin of surface stress, on the atomic scale, derives from the crystalline structure. The epitaxial layer, or surface atoms, reside in a lower electron density and therefore a different equilibrium spacing than the bulk. The bulk atoms force the surface atoms to fit into the epitaxial overlayer of the crystalline substrate. As a result, the surface atoms are strained by the bulk, leaving the surface stressed by the underlying lattice [2].

#### Strain Dependency of Surface Stress in Traditional Solids

Although surface tension is most familiar in liquids, it is a property shared by solids as well. In contrast to liquids, when a surface of a solid is elastically stretched, the number of atoms per unit area changes, such that generally  $\gamma \neq \Upsilon$  in solids [2]. The relationship between surface energy and surface stress can be derived through the use of the elastic deformation tensor  $\epsilon_{ij}$ , where  $i, j = 1, 2$ . We can then define  $d\epsilon_{ij}$  to be an infinitesimal and elastic (reversible) strain as a result in a variation of the surface area,  $A$ . The surface stress tensor,  $\Upsilon_{ij}$ , is the work associated with the variation in the excess free energy of the surface due to strain,  $\gamma A$ . Thus, we can write,

$$d(\gamma A) = A\Upsilon_{ij}d\epsilon_{ij}$$

Expanding out the first term,  $d(\gamma A) = \gamma dA + Ad\gamma$ . Utilizing symmetries, we can say that  $dA = A\delta_{ij}d\epsilon_{ij}$ , where  $\delta_{ij}$  is the Kronecker delta. Making the substitution, we find

$$\gamma dA + Ad\gamma = \gamma A\delta_{ij}d\epsilon_{ij} + Ad\gamma = A\Upsilon_{ij}d\epsilon_{ij}$$

And thus,

$$\Upsilon_{ij} = \delta_{ij}\gamma + \frac{\partial\gamma}{\partial\epsilon_{ij}} \quad (1.1)$$

This is known as the Shuttleworth Equation (1.1), and clearly shows that both  $\gamma$  and  $\Upsilon$  in solids are dependent on the strain state of the material.

Experimental measurements of surface stress have been around as early as the 1960, though measurements of strain-dependent surface stress have only been attempted much more recently and returned scant results [5, 6, 7, 8, 9]. Metals are an incredibly useful building tool due to their strength<sup>1</sup>, but their stiffness<sup>2</sup> also makes measuring properties as a function of strain severely limited, as most metals will fracture after a few percent strain.

For most solids, these surface effects go unnoticed in everyday life due to the overpowering effects of the bulk's elasticity compared to any surface energies.

See Nat  
Comm 2017  
ref 7-12

### 1.2.3 Surface Stress Effects in Soft Solids

For solids of small enough size or soft enough composition, the surface energies can compete with or even dominate the effects of the bulk, resulting in strange and counterintuitive physics. For example, the addition of finite, microscopic, liquid droplets in a soft solid actually stiffens the material [10], and stiffening micropillars are far stiffer than conventional physical theory predicts.

Include 3-phase zoom graphic

Revise af-  
ter reading  
papers

Not toally sure what KEJ wants me to talk about. Would like ask in person.

- Contact Lines zoom in
- Liquid inclusions
- Rayleigh Plateau
- Instability
- Rounding corners
- adhsion (many?)

Early observations of  $\Upsilon$  in soft solids came from consiering the wetting behavior of liquid droplets on soft solid surfaces. The traditional Young-Dupre' picture of wetting is shown in Figure 1.1. This is clearly an unbalanced force diagram in vertical direction; the only vertical force component drawn is the liquid-vapor surface tension,  $\gamma_{lv}$ . The normal force from  $\gamma_{lv}$  must be balanced by the elastic substrate's resistance to deformation. Calculating this value, however, is still an open question. According to continuum elastic theory, the stress exerted by  $\gamma_{lv}$  on the solid diverges at the contact line [11]. While Contact Mechanics dates back to the 18th century, seemingly simple problems like a liquid droplet on an elastic surface are still not yet well understood and provide challenging question when inspecting on a small enough scale.

*The increased importance of surface stress in this regime leads to some material properties that are counter-intuitive to our everyday experiences. For example, soft solids can be stiffened with the inclusion of pockets of fluids below the elastocapillary length. In this regime, the surface tension dominates. And thus, the inclusion of a hole, while removing material affects the elastic stiffness, it also increases the surface area of the substrate. In*

---

<sup>1</sup>Strength: the maximum force per unit area a material can withstand

<sup>2</sup>Stiffness: the material's resistance to deformation via strain

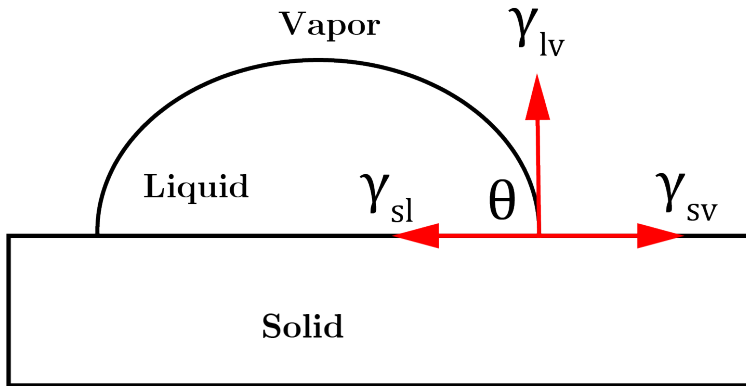


Figure 1.1: Classical Three-Phase Diagram]

*this regime, this increase in surface area is more important, and thus leads to a solid of increased stiffness.*

Jerison et al. 2011 [11] found modeling the deformation of the elastic substrate due to a liquid droplet fit best with a model that incorporated both the finite thickness and surface tension of the substrate. This new model solved many issues with the previous best solution by Boussinesq: taking into account the finite thickness ensured that the deformations would go to zero far from the contact line, and the substrate's surface tension resolves the single stress singularity, eliminating the divergence of strain and vertical displacement at the origin. Additionally, Jerison found that there must be a large discrepancy in  $\gamma_{sv}$  and  $\gamma_{sl}$ , which were previously assumed to be identical.

I re-read Jerison 2011. I misread it the first time. In doing their calculations, they assumed the contact angle was close to 90 deg, and they assumed  $\gamma_{sl} = \gamma_{sv}$ ...but their theory doesn't account for contact angles far from 90 deg....which are the instances in which  $\gamma_{sl} \neq \gamma_{sv}$ . Remove this last sentence.

#### 1.2.4 Direct Measurement of Solid Surface Stresses

Theoretical calculations for surface stress generally involve the taking the derivative of the predicted surface free energy with respect to strain. Various methods for metals involve calculating the electronic density, the kinetic energy, and the electrostatic exchange-correlation<sup>3</sup> [12].

Measuring the surface stresses even in soft solids has proved experimentally challenging over the years. A modern method of measuring the deformation of a soft, elastic solid imposed by the liquid droplet in Figure 1.1 was introduced by Jerison in 2011 [11] and later utilized by Style *et al.* in 2013 [13]. They measured the 3-phase contact line geometry in

(Cite a few things here?)

<sup>3</sup>Forgoing the independent electron approximation, the electronic exchange is a measure of deflection due to the presence of other electrons

figure 1.1 without requiring any prior knowledge about the bulk elastic properties of the substrate material.

*While this technique is effective, it is limited in its applications due to material properties. The method only works for immiscible fluids such that the gel does not absorb the surface droplets. Furthermore, the fluid must also have a low volatility; otherwise, the droplet would begin to evaporate while waiting for the surface deformations to settle.*

### Puzzling Surface Stress Measurements in Gels

In contrast to hard materials, it has been widely assumed that the surface stress in soft matter would be nearly strain-independent. Gels, for example, are comprised mainly of a fluid phase trapped between a solid mesh of polymers<sup>4</sup>. Because the surface stress in liquids is constant and equal to the surface energy of the substance ( $\Upsilon = \gamma$ ), it was largely assumed that deforming a gel would not have a significant effect on the surface tension, given that the fluid could flow back to the stretched surface of the gel.

In the following years, further tests of surface stress in soft solids (Table 1.1) were measured with wildly varying results. It began to become clear that the surface stress of soft solids was not simply that of the fluid phase, and there is more to the mystery.

Silicone	Young's Modulus (kPa)	Measured $\Upsilon$ (mN m <sup>-1</sup> )	Reference
Sylgard 184	770	19	[14]
Gelest	5.6	20	[15]
Sylgard 184	2400	26	[16]
Dow Corning CY52-276A/B	3	30	[13]
Sylgard 184	18	30-70	[17]
Sylgard 184	1000	40-50	[18]
Dow Corning CY52-276A/B	3	42-59	[19]

Table 1.1: A Collection of Previously Measured  $\Upsilon$  Values

While gels are technically classified as solids, they exhibit many properties that are more closely associated with liquids. Most notably, gels are comprised mainly of fluid (by weight). Their rigidity is the result of a three-dimensional network of crosslinked molecules which entrap large amounts of liquid throughout via capillary forces. The result is a solid whose stiffness is determined by the composition and temperature. Surface stress in soft solids is a topic of growing interest. Unlike in metals, elastocapillary physics plays a crucial role in determining the material's behavioral properties. In 2011, Jerison et. al [11] found that deformations of a silicone substrate due to a liquid droplet on the surface required the inclusion of surface tension. Furthermore, they determined that  $\gamma_{sl}$  and  $\gamma_{sv}$  must be dramatically different from one another, despite the previous assumption that the terms would be equal.

---

<sup>4</sup>For a more in depth explanation, see section 4.1

Soft solids provide a unique opportunity to measure strain-dependent surface stress. Despite being a solid, soft solids, such as gels, can easily be stretched elastically. In 2017, Xu, Jensen et. al published a paper [1] making the first direct measurement of strain-dependent surface stress in solids. Their measurements suggest a surprisingly strong linear relationship between surface-stress and strain, measuring that the surface stress of their PDMS substrate more than doubled at 20% strain. *To measure the surface stress of the material, the group utilized Jerison's 2011 method [11]. First, a glycerol or flurinaeted oil droplet is placed atop a soft, elastic silicone gel substrate. To measure surface deformations, the substrate is first coated with fluorescent beads, which can subsequently be measured using confocal microscopy. The located positions of the fluorescent beads outline the surface and allows for reconstruction of the surface deformations.* Additionally, their method of measurement is limited to a select combination of materials. We have developed a method for measuring strain dependent surface stress that is applicable to a wide variety of stretchable, soft materials. To provide greater evidence of strain dependent surface stress, we made a separate measurement in PDMS as well as a variety of other soft materials using soft adhesion. In this thesis, I present the full background, methods, and underlying physics of the process.

stretchable/  
soft redundant?

### Surface Tension and Contact with Soft Elastic Solids

Over the last few years, there has been a significant amount of work regarding adhesion in soft solids. We want to take advantage of what is known about the role of surface stress in the contact mechanics of soft solids to directly measure the surface stress while varying the properties of the underlying substrate. In doing so, we will have created a new form of measuring strain-dependent surface stress, applicable to a broad array of stretchable materials. The contact angle based method used in the first direct measurement of  $\Upsilon(\epsilon)$  [1] is limited to a select combination of materials, as the liquid droplet must be immiscible and non-volatile. We hope to apply Jerison's 2011 technique to stretchable substrates in order to measure  $\Upsilon(\epsilon)$  for a wider variety of materials. The specifics of this technique are covered in the following chapter.

### 1.3 Outline of the Thesis

This thesis begins with a derivation of modern theory of contact mechanics for soft solids. With this in mind, we proceed to outline the experimental design and setup in chapter 2, followed with an example of data aquisition and image analysis in chapter 3. Chapter 4 contains our preliminary surface stress and adhesion results for various materials. Finally, chapter 5 looks ahead, discussing possibilities for future experiments and improvements to the experimental process.

# Chapter 2

## Experimental Approach: Setup, Data Acquisition, & Analysis

In this chapter we discuss the setup of the experiment from start to finish. First we discuss the underlying theory required for the technique. Next, we walk through the walk through the experimental setup, the process of acquiring data and processing it for a single sphere. Finally we address the stretching apparatus, including its calibration process, and analyzing the results. Further details can be found in the appendices.

### 2.1 Measuring Surface Stress via Adhesion

#### 2.1.1 Beyond Hertzian Mechanics and JKR Theory

Hertzian Mechanics, developed by Heinrich Hertz in the 1800's, allows for the calculation of stress and deformation based on the elastic moduli of the contacted surfaces, as well as their radii of curvature and applied force. While Hertzian mechanics stood for a long time, it neglected to take into account the adhesion energy of the system.

In 1971, Johnson, Kendall, and Roberts (JKR) sought to remedy this omission by developing a classical theory of contact mechanics that balances the forces of adhesion with elasticity from the bulk and the surface free energy [20]. Today, it is still the standard theory used to interpret and soft contact situation. However, it has recently been shown that while JKR theory is a great improvement over Hertzian Mechanics, it breaks down in the elastocapillary regime. Specifically, at lengths where

[add citation]

$$L_c \leq \frac{\Upsilon}{E} \quad (2.1)$$

the surface energies compete with those of the bulk and can no longer be ignored. Fittingly,  $L_c$  is referred to as the elastocapillary length. By understanding the role of surface tension in soft adhesion, we can measure the physical properties of a balanced system in the elastocapillary regime and hence measure the surface stress and adhesion energy from the balance of forces.

### 2.1.2 Force Balance Derivation

When materials are soft or small enough, three main forces balance to determine the contact mechanics of the system. Consider a marble sinking into a soft, sticky substrate. Adhesive forces increase the contact area between the marble and the substrate. Increasing the contact area has the effect of “pulling” the marble into the gel. As a consequence, the substrate is being compressed [vertically], which is counteracted by the elastic forces within the bulk. This compression also has the effect of stretching the surface of the substrate, which is counteracted by substrate’s surface tension. Below, we calculate the energy term associated with each of the forces acting on a dense sphere sinking into a soft substrate.

Move to later in chapter: For a silica microsphere, we can ignore the weight of the sphere when calculating the elastic energy term. The force of gravity on the microsphere is negligible compared to the other forces. The density of silica (silicon-dioxide) is 2.65 g/cm<sup>3</sup>. For a very large sphere with radius (or is this diameter...) 50 microns, gravity applies a force of roughly 1.02e-08 N.

#### Elastic Energy

The energy required to make a circular indentation of radius R and depth d can be derived from Hertzian contact mechanics [21, 22, 23]. Contact between a sphere and an elastic half space<sup>1</sup> is a classic Hertzian contact problem. It is easiest to calculate the force and then integrate to determine the potential energy. For two elastic surfaces in contact with no externally applied forces, the force from elastic contact is:

$$F = \frac{4}{3} E^* R^{1/2} d^{3/2} \quad (2.2)$$

where

$$\frac{1}{E^*} = \frac{1 - \nu_{sphere}^2}{E_{sphere}} + \frac{1 - \nu_{substrate}^2}{E_{substrate}}$$

For a glass sphere sinking into a soft substrate,  $E_{sphere} \gg 1 - \nu_{sphere}^2$ , so this first term can be dropped as a reasonable approximation<sup>2</sup>. Thus we can approximate  $E^* \approx \frac{E_{substrate}}{1 - \nu_{substrate}^2}$ . Substituting this into equation (2.2), we find:

$$F \approx \frac{4}{3} \frac{ER^{1/2}d^{3/2}}{1 - \nu^2} \quad (2.3)$$

Because  $F = \frac{\partial U}{\partial d}$ , we can simply integrate equation (2.3) to obtain the energy relation:

$$U_{elastic} \approx \frac{ER^{1/2}d^{5/2}}{1 - \nu^2} \quad (2.4)$$

---

<sup>1</sup>i.e. the contact area is  $\ll$  the characteristic radius of the object. A flat plan can be thought of as  $R = \infty$

<sup>2</sup> $\nu_{SiO_2} \approx .17$  and  $E_{SiO_2} \approx 70 \times 10^9$  Pa

## Adhesion Energy

The energy of adhesion is  $W$  multiplied by the surface area in contact (as found above). Namely,

$$U_{\text{adhesion}} \approx -2\pi WRd \quad (2.5)$$

where  $W$  is the adhesion energy.

I think I should explain adhesion somewhere and talk about the Dupre equation 1869.

Not sure where I want to put this, however. Maybe some of this stuff and the derivations should actually be in chapter 1. Also “energy of adhesion = const. \* adhesion energy” lol hmmm

## Surface Energy

$\Upsilon$  is the surface stress, which is equal to the energy cost per unit area required to create surface via cutting or stretching the material. For a flat substrate being stretched via the indentation of a sphere, the energetic cost is

$$U_{\text{surface}} = \pi \Upsilon_{sv} \Delta A \quad (2.6)$$

where  $\Delta A$  is the change in surface area when stretched by part of an indenting sphere (spherical cap). Determining the change in area is a simple geometrical problem.

$$\Delta A = A_{\text{cap}} - A_{\text{circle}}. \quad (2.7)$$

Let  $a$  be the base radius of the circle projected on the plane of the substrate's surface. Let  $R$  be the radius of the indenting sphere, and  $d$  be the depth into which it is stretching. We can find a relationship between these variables using the Pythagorean theorem.

$$\begin{aligned} a^2 + (R-d)^2 &= R^2 \\ a^2 + R^2 - 2Rd + d^2 &= R^2 \\ a^2 &= 2Rd - d^2 \\ a^2 + d^2 &= 2Rd \end{aligned}$$

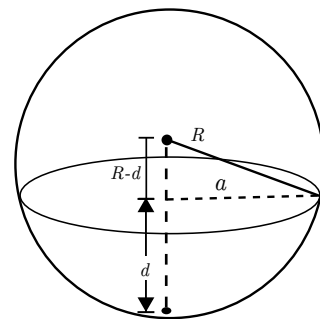


Figure 2.1:  
Spherical  
Cap  
Geometry

Now, solving for  $\Delta A$  and using the above relationship in the last step, we find:

$$\begin{aligned} \Delta A &= 2\pi R d - \pi a^2 \\ &= \pi(a^2 + d^2) - \pi a^2 \\ &= \pi d^2 \end{aligned}$$

Rewriting (2.6), we can simplify surface energy in this geometry as

$$U_{surface} = \pi \Upsilon_{sv} d^2 \quad (2.8)$$

### Force Balance

At static equilibrium, the sum of the energies is:

$$U_{total} = \Upsilon_{sv} \pi d^2 + \frac{cER^{1/2}d^{5/2}}{1 - \nu^2} - 2\pi WRd$$

where  $c$  is a geometric factor to be determined in the next step. We can re-arrange the equation such that the sum of forces is equal to zero and differentiate both sides with respect to depth.

$$\begin{aligned} \frac{\partial U_{total}}{\partial d} &= \Sigma F = 0 \\ 2\pi\Upsilon_{sv}d + \frac{5cER^{1/2}d^{3/2}}{2(1 - \nu^2)} - 2\piWR &= 0 \end{aligned} \quad (2.9)$$

Where  $c = \frac{8}{5\sqrt{3}}$ . This value of  $c$  is chosen to recover classical JKR theory, which predicts an indentation of  $d = \left[ \frac{\sqrt{3}\pi W(1-\mu^2)}{2E} \right]^{2/3} R^{1/3}$  [22, 20]. This energy balance was first published in 2013 by Styles et al. in *Nature Communications* [22].

Why did you want me to mention Jensen PNAS 2015? Wasn't this the phase separation paper? What connection were you thinking I should make here?

### 2.1.3 Experimental Approach

Equation 2.9 gives us a quantitative relationship between the spontaneous indentation depth,  $d$ , sphere radius,  $R$ , and key material properties:  $\Upsilon$ ,  $E$ ,  $\nu$ , and  $W$ . The Young Modulus,  $E$ , and the Poisson ratio,  $\nu$  of the substrate can be measured separately for the substrate material. The depth  $d$ , and the radius  $R$  of the sphere can be measured using fluorescent confocal microscopy, as described in section 3.1. The only remaining terms,  $W$  and  $\Upsilon$ , the adhesion energy and the surface stress, respectively, can be determined with a two-parameter fit of  $d$  vs.  $R$ .

move to ch 5: Alternatively, it is possible to measure the adhesion energy separately. This technique, though not critically important to the experiment, is of interest and exploring if not just for the benefit of adding the capability to the lab.

## 2.2 Preparing a Substrate

In the following section, we outline the process of preparing a soft substrate for testing. The process is similar for a zero strain sample and a stretchable sample, and we make clear any distinctions between the two processes. Specific details for our substrate types can be found in Chapter 4.

Before preparing the substrate, we prepare the surface on which the substrate will be held, from hereon referred to as the underlayer. For a non stretched sample, we use a glass coverslip, and for a stretched sample we use a thin PDMS sheet. We first coat this layer with fluorescent beads in order to later locate the bottom of our substrate. In preparing our substrate, there are two important factors to consider: thickness and evenness of the surface. The substrate must be thick enough such that the indenting spheres do not feel a measurable force from the glass or PDMS underlayer. This bottom layer of fluorescent beads allows us to easily gauge the thickness of our substrate. It is important that our substrate has an even surface, otherwise it is difficult to determine the sphere's depth,  $d$ . To achieve this, we use a technique called spin-coating where we place our uncured substrate (when it still has liquid like viscosity) on the underlayer and spin it rapidly for a period of time. The angular momentum causes the flings the fluid away from the center of the underlayer. The result of this process is an even coating which will cure into our substrate over the next day.

Once cured, we deposit a second layer of fluorescent beads on the surface. These act as tracer particles which outline the indentation sphere. Using fluorescent confocal microscopy, we are able to precisely locate each fluorescent bead and outline the indentation sphere. It is important that the beads are dense enough to give a high resolution, yet not so dense as to become indistinguishable; this presents a challenge the MATLAB particle locating software. For a stretchable sample, we place the substrate, now cured onto the stretchable PDMS underlayer, onto the lubricated stretching apparatus. It is important remove any small bubbles on the stretcher's ring to ensure an airtight seal.

The final preparation step is to sprinkle silica spheres of a range in size on top of the silicone. This should be done at least 30 minutes before collecting data so that the spheres have time to settle into an equilibrium state into the silicone. From a side view, the final setup should look like Figure 2.2.

I don't like underlayer name. Base plate? Substratum base?

## 2.3 Stretching Apparatus

Our interest is not just in measuring,  $W$  and  $\Upsilon$  for a given substrate, but in understanding how those values change when under strange As needed, we have built our own equibiaxial stretching apparatus capable of maintaining up to 35% strain in our silicone samples. The design is based off of previous work designed for stretching biological tissues [24] and is similar in design to the apparatus used in the 2017  $\Upsilon(\epsilon)$  measurements [1]. Below is a general description of the design, though detailed design documents can be found in Appendix A.

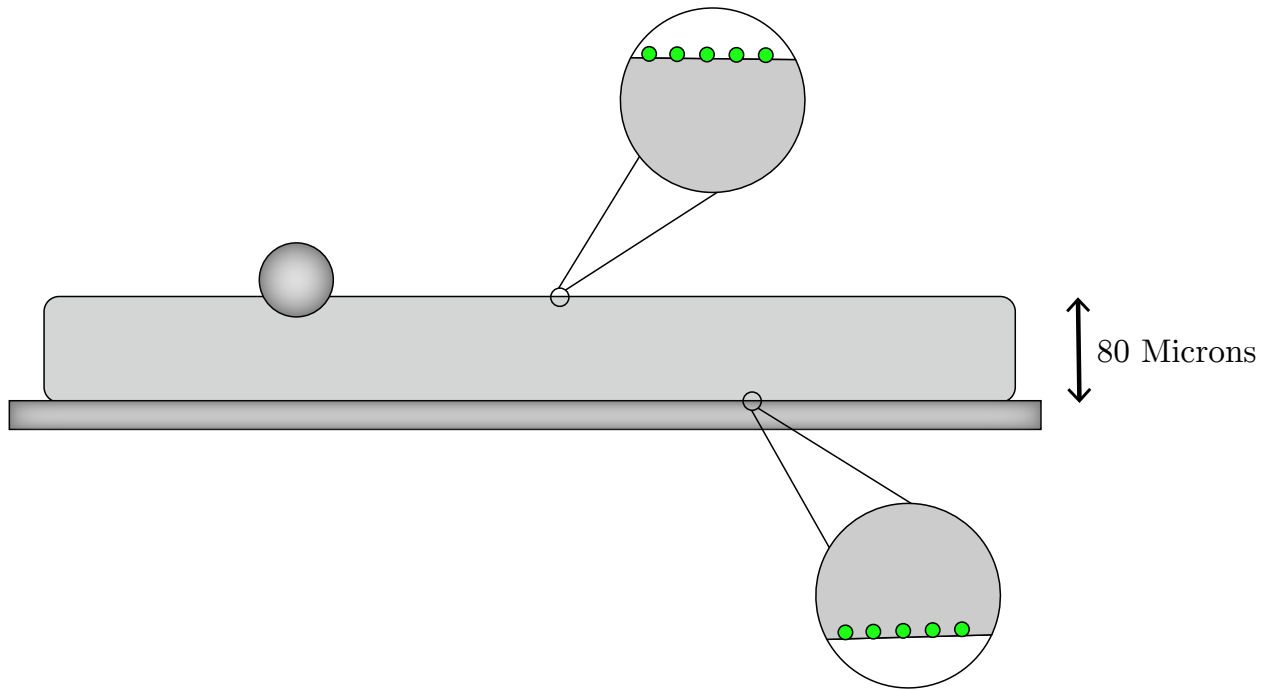


Figure 2.2: Above is the side profile of a prepared substrate sample. There are two layers of fluorescent beads: the bottom layer is used to measure the substrate's thickness, and the surface layer is used to outline the profile of the larger, indenting sphere. The soft substrate sits on an underlayer, namely glass or a stretchable PDMS silicone.

### 2.3.1 Stretcher Design

Geometrically, the stretching apparatus is constructed of two concentric cylinders connected at the base to create a channel between them. The top of each ring is flat, apart from a slight chamfer to reduce the risk of ripping the sheet as it is stretched. Each ring is then coated in Dow Corning vacuum grease to make a seal. It is critical that the inner ring has an ample amount of grease so that when a vacuum is pulled in the channel, the sheet will stretch from the center outwards and not from the edges inwards. The sheet is held in place with an o-ring wrapped around the outside of the cylinder, which is then clamped down by a removable outer ring using a tension clamp. The tension provided by the o-ring and clamp ensure that a solid vacuum is kept and the edges of the sheet are minimally stretched into the trough.add to appendix?

A tapped screw hole on the side of the apparatus connects the chamber to a syringe via thin, plastic tubing. To pull a vacuum in the channel, we withdraw air using a syringe pump. This allows us to have a consistent withdraw rate and control over the amount of air withdrawn to a high degree of precision.

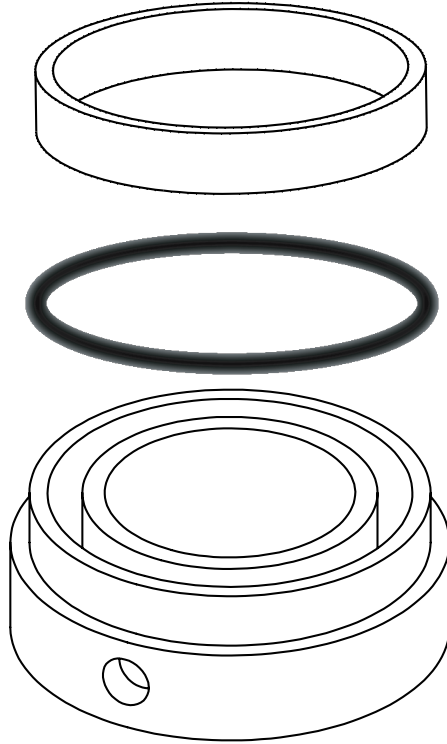


Figure 2.3: Here is an exploded view of the stretching apparatus. The substrate goes on top of the base (substrate side down). It is then held down with an o-ring, which sits on the outside ledge. A second ring sits on top of the o-ring and is then held down by the microscope mount (not pictured here).

## 2.4 Calibration

Originally, we intended to calibrate the strain value induced by the vacuum to the extent that we could predict the induced strain based on the amount of air withdrawn from the stretching apparatus. We withdrew air from the syringe and measured the movement of glass spheres adhered to the surface using a 10x air lens on our Nikon confocal microscope. Using the transmission detector allowed us to image the surface of our material with a wide field of view. Strain percentage was calculated using MATLAB code [1].

There are several obstacles in calibrating the induced strain. First, the stretching apparatus works best when a large strain is applied. Applying small strains one after another works but there is a threshold to induce stretch. No stretching change is visible if less than 2ml is withdrawn from the cylinder per increment. Thus, there is a limited resolution to our calibration data, which would not be a problem if the strain was linear. However, preliminary measurements indicated that the applied strain was nonlinear. This agrees with the previous results [24] obtained using a similar device. *note to self, double check this is where that graph I'm thinking about actually showed up.* Lastly, the greatest problem with calibrating strain is that we change substrates often. Even if we were to use the same exact

Better/more citations for strain code?

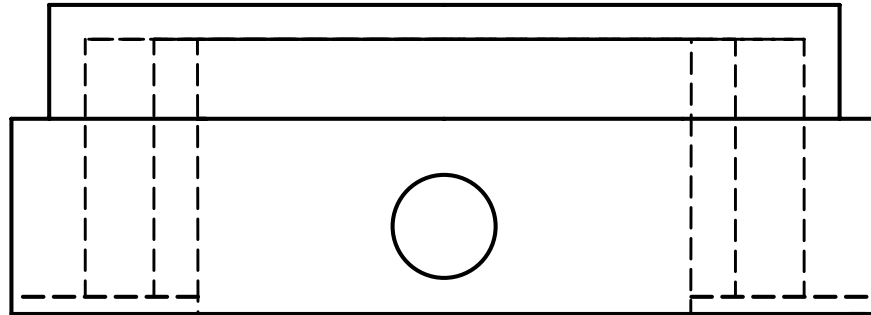


Figure 2.4: Above is the side profile of the stretching apparatus. Note the channel attached at the base, and the large center hole at the base where our substrate can be accessed by the microscope.

sample, by removing it and setting up the device again, there is no way to standardize a zero-applied strain point. To prepare the stretching device, the sample is placed over the opening and a rubber o-ring is placed around the sample to help affix it in place. The sample must then be stretched and wiggled around slightly to remove any snags that could jeopardize the vacuum's efficacy. This means that every time a new sample is prepared, it is in an unknown and unique state of induced strain. It could even have less than zero strain if the sample is loose in large center opening *Think of better name for this*.

It was thus determined best to measure strain every time we applied a new strain to the silicone substrate and compare it to the substrate's original state. This also assured us that we knew the correct strain value to a higher precision for any given data set. Additionally, with the pleasantly unexpected ability to hold strains exceeding 30%, the  $2\mu\text{m}$  resolution limit became superfluous in seeking to measure  $\Upsilon(\epsilon)$ .

### 2.4.1 Measuring Strain

To determine the induced strain, we maximized the field of view. This allows us to see how more spheres are shifting, and thus gives a more accurate estimate of induced strain. As such, we decided to switch to the bright-field and measure how the spheres were shifting when stretched. We used a 10x air lens in conjunction with the transmission detector on our Nikon Confocal. We adjust the settings to give decent contrast, but it is more important to have the spheres in focus. For our Nikon this usually means setting the Power (HV) to 80. Each sphere reflects light, and it is this reflection that our particle locating software tracks after some image processing. An example image is located below (Fig.2.5), next to the same image after adjusting the contrast to help our tracking software with particle locating:

To track how the substrate stretches, we first find a centrally located group of spheres, or “constellation.” A good constellation is one that easily identifiable for relocation and tracking purposes, and one that has many discrete points in the field of view - i.e. there are plenty of non-overlapping spheres. *It is an added bonus to find 4 spheres perpendicularly located, such that they form the tips of cross.* Though not necessarily, this is useful for a preliminary

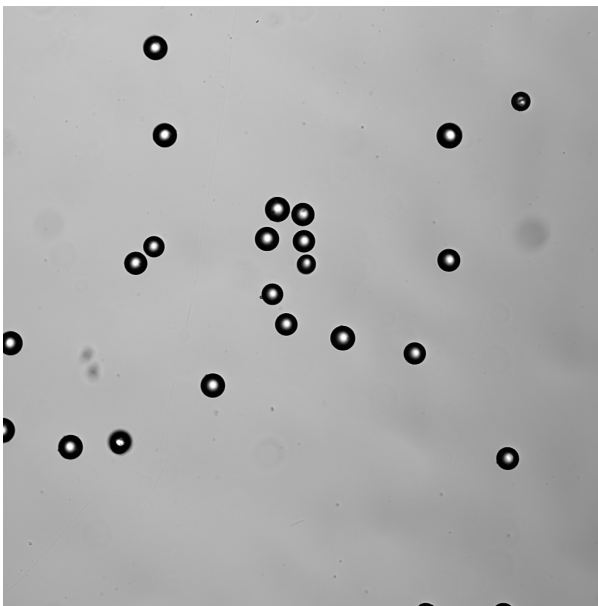


Fig. A

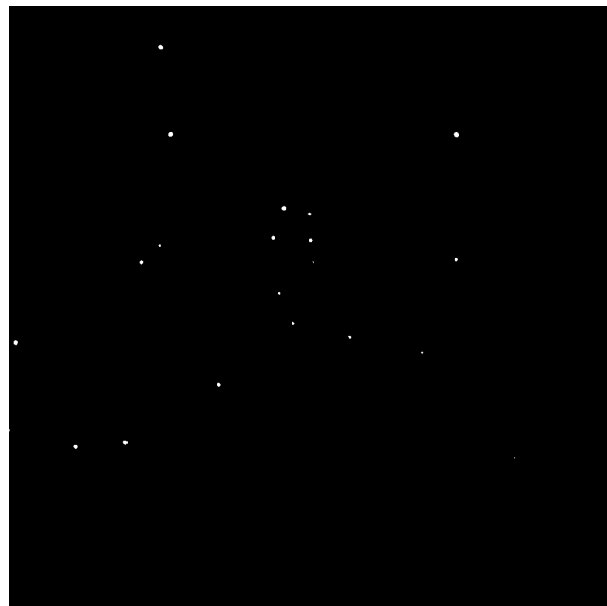


Fig. B

Figure 2.5: Figure A shows the calibration constellation before any strain is applied. Fig. B shows the same image after processing. Only the sphere reflections remain.

strain calculation using the built in measuring functions on the Microscope's software. It is nice to track the progression of stretching and ensure the substrate is not preferentially stretching in one direction; this could indicate the substrate is caught in the apparatus. Not only does this ruin the symmetry assumptions being made for our calculation, but it could lead to the substrate tearing if more strain is being applied than expected.

To evacuate the cylinder, we use the Harvard Apparatus<sup>TM</sup> Elite Pro Syringe Pump with a 50ml Luerlock syringe. Before beginning any stretching, we withdraw a few ml of air to ensure the substrate is flat and not sagging. At this point we take a picture of the brightfield and call it the "zero applied strain" image. We compare all stretched data to this image in order to determine the induced strain. Because of the geometry of the stretching apparatus, along with the way the silicone cures, it is difficult *impossible??* to determine the true strain of the silicone. However, we are most interested in the slope of the  $\Upsilon$  vs.  $\epsilon$  curve,  $\Lambda$ , so this is not vitally important.

The induced strain is a tensor of rank two. *If I'm bored and have time, I'd like to add an appendix to talk about this tensor. I think that would be the best way for me to really understand it. That graphic in the book hasn't really stuck with me* Because we are stretching the substrate equally in all directions, we can just look at the magnitude of the tensor and treat the strain as a scalar.

There's an alternate image where each point is an x for before after. Replace figure with that and zoom in on sphere cluster.

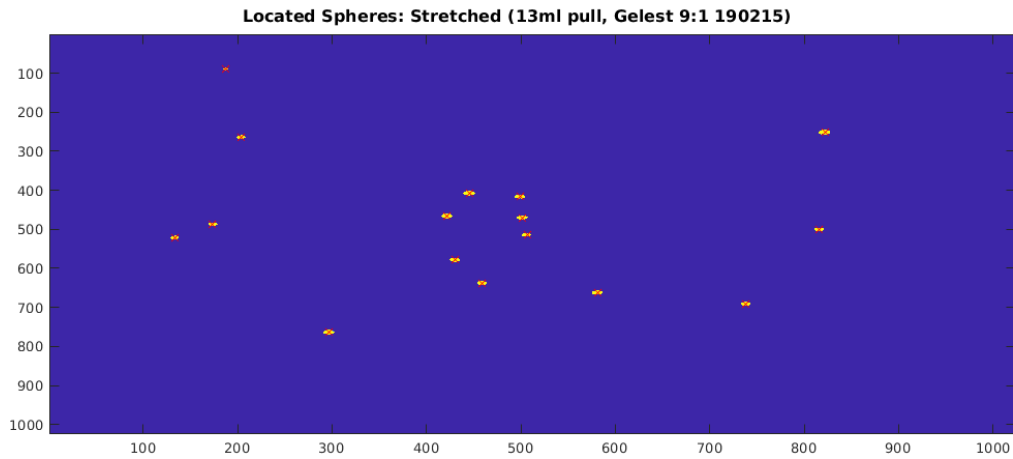


Figure 2.6:

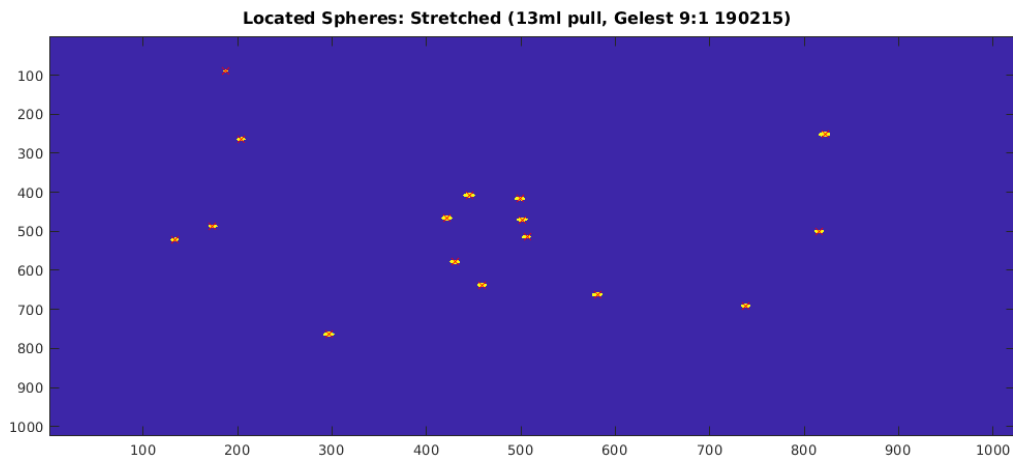


Figure 2.7: These are placeholders for now. I don't really like how they look and I don't think they're totally necessary. It might be nice to keep them if I can clean them up. Especially if I get some nice stretch data with the new DC

## 2.5 Material Characterization

To measure the stiffness of our substrate, we do not use the confocal measurement sample. Instead, when preparing the sample, we cure a surplus of the substrate material in a vial to test the bulk characteristics of the sample.

We take a standard bulk stiffness measurement using the texture analyzer. A rigid cylinder with radius  $R = 1.5$  mm is slowly indented into the bulk substrate. The force response vs. indentation depth is recorded for several tests with varying starting heights and locations (See Figure 2.8). We use the average E value obtained from these tests in our W, Y

fitting. The fitting process will be reviewed in Chapter 3.

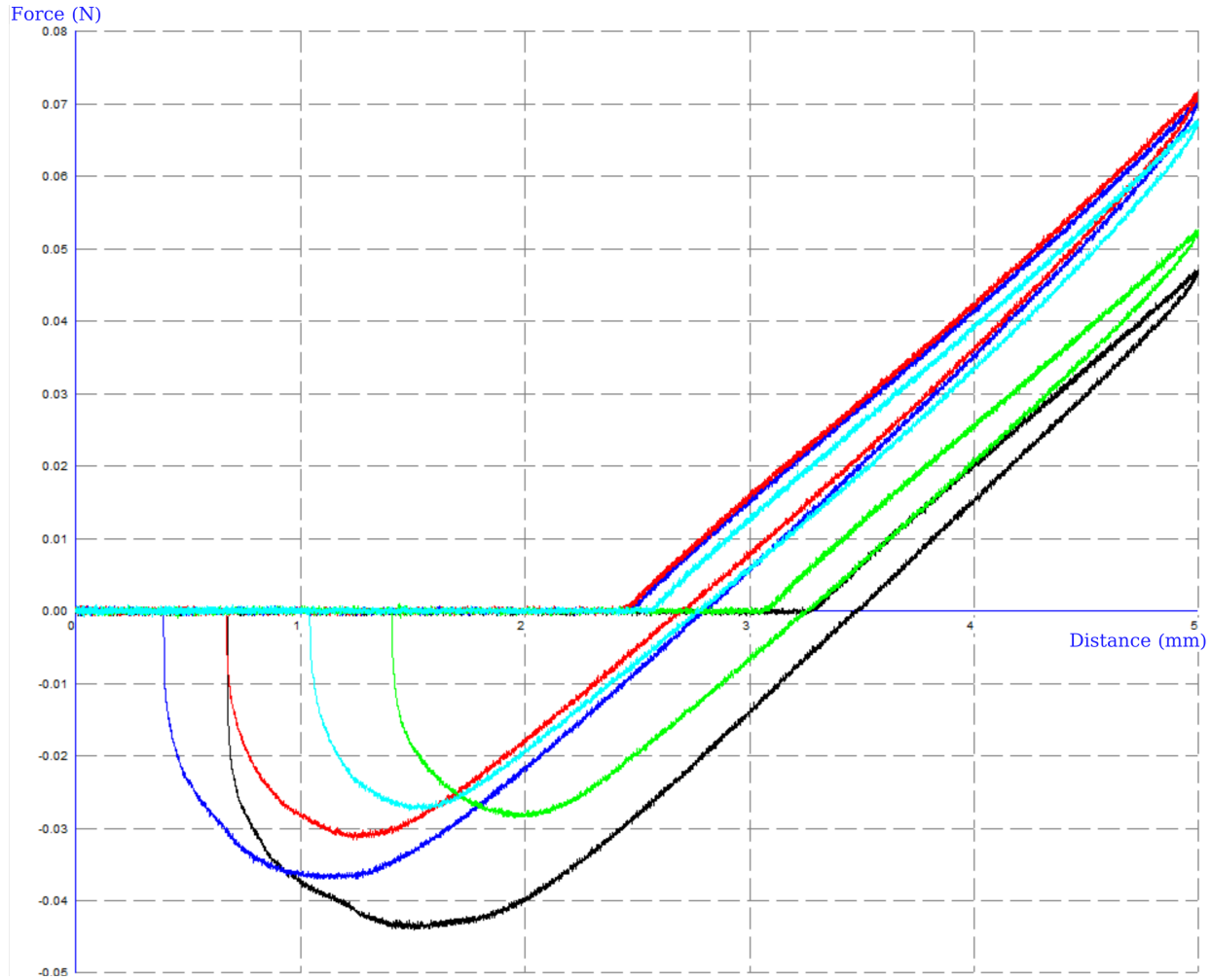


Figure 2.8: Force vs indentation depth for a bulk sample of silicone. Each color represents a separate measurement at varying starting heights and locations on the sample.

Do you think the axis values are too small? I haven't seen this printed yet.

### 2.5.1 Hertzian Contact Mechanics Derivation?

We calculate the Young's modulus for the bulk sample using classic Hertzian Contact mechanics between a flat, rigid cylinder and an elastic half-space.

$$F = 2RE^*d \quad (2.10)$$

where

$$\frac{1}{E^*} = \frac{1 - \nu_1^2}{E1} + \frac{1 - \nu_2^2}{E2}$$

For Silicone,  $\nu \approx .5$  for low strains; for the rigid cylinder,  $E \gg 1 - \nu^2$ , so we can ignore that term. From the Force vs. depth information, we can write an equation for E.

$$\frac{1}{E^*} = \frac{2Rd}{F} \quad (2.11)$$

$$\frac{1 - \nu^2}{E} = \frac{2Rd}{F} \quad (2.12)$$

$$E = \frac{(1 - \nu^2) F}{2Rd} \quad (2.13)$$

$$E = \frac{(1 - .5^2) F}{2(1.5 \times 10^{-3})d} \quad (2.14)$$

Equation alignment doesn't look right

## 2.6 Putting it all Together

Using the texture analyzer, we can measure  $E$  and  $\nu$  for our substrate. We can then use confocal fluorescent microscopy to measure  $d$  vs.  $R$  for many sphere per sample. We can then run a two parameter fit using this Equation 2.9 to determine  $\Upsilon$  and  $W$ . Using our equibiaxial stretching apparatus, we can repeat the  $d$  vs.  $R$  measurements at a range of strain to determine  $\Upsilon(\epsilon)$ . The process of collecting the  $d$  vs.  $R$  measurements for a single sphere is explained in Chapter 3.

# Chapter 3

## Data Acquisition and Image Analysis

### 3.1 Fluorescent Confocal Microscopy

Confocal Microscopy is a technique capable of probing a sample with true 3-Dimensional optical resolution. The technique works by only allowing in focus light through a pinhole. By changing the plane of focus, one can traverse an object azimuthally or reconstruct a full three-dimensional image by compiling a “stack” of these images.

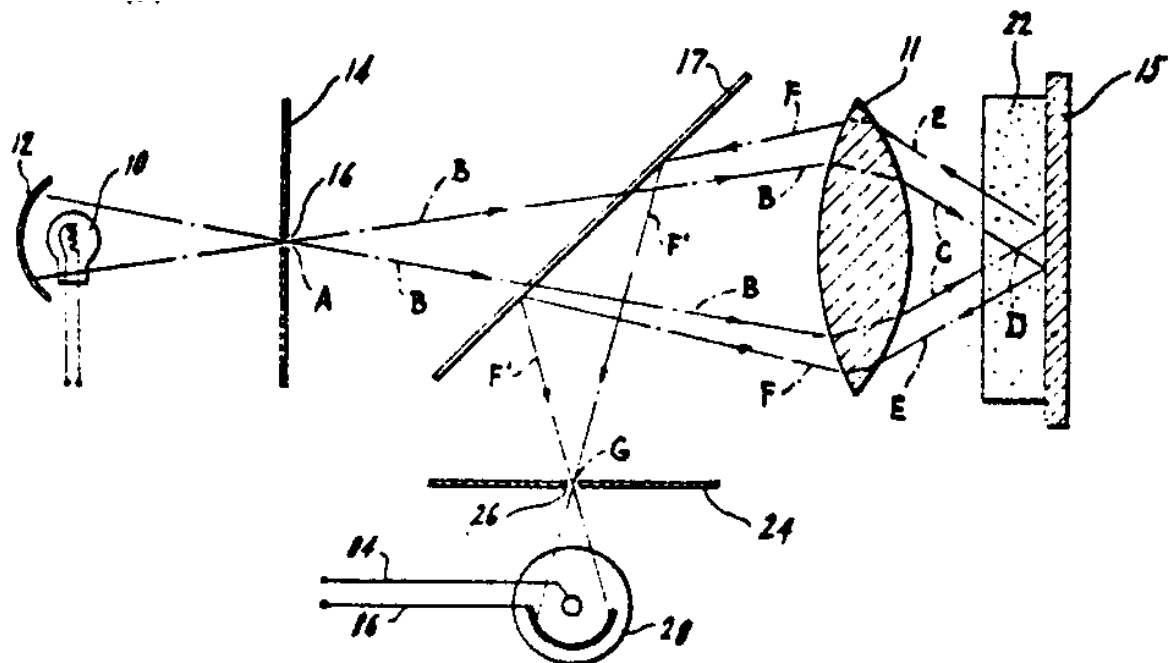


Figure 3.1: Above is a diagram from Marvin Minky's classic 1961 patent [25] for a confocal microscope. A pinhole before the photodetector blocks the out of plane light.

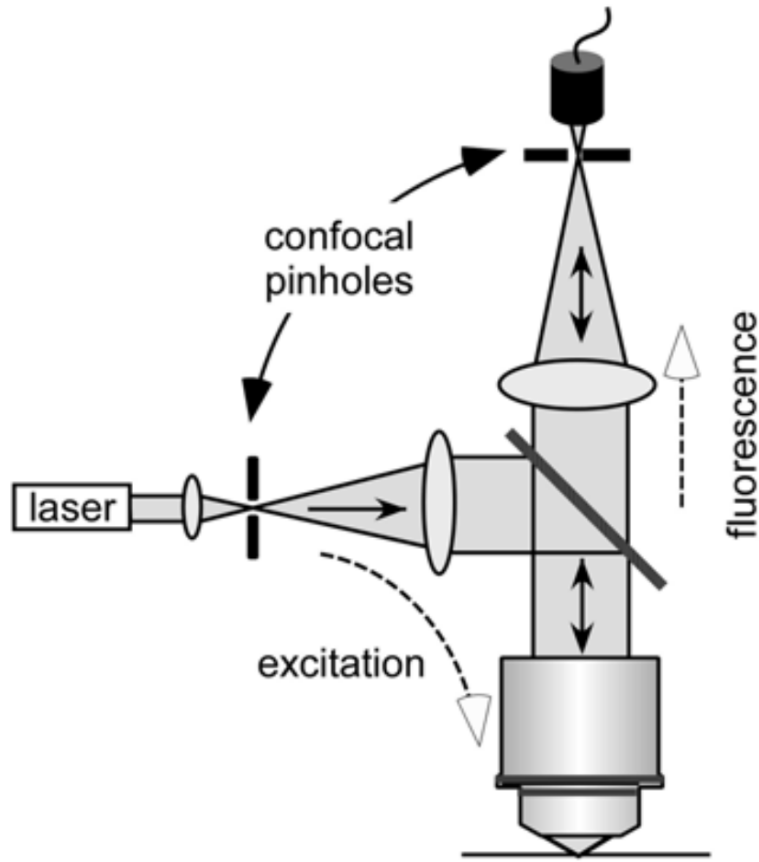


Figure 3.2: In fluorescent confocal microscopy, a diachroic mirror is used to separate the laser light from that emitted by the excited fluorophores.

cite or make own for this diagram.

Fluorescent Confocal Microscopy works by the same general principle, only with the added complexity of optically-exitable fluorophores. These fluorophores absorb light from a narrow range of frequencies and re-emmit fluorescent light at a different known and specific frequency, which can then be measured. This allows for a greater resolution to larger objects, as well as the ability to detect objects that would otherwise be invisible to the microscope.

Fluorescent Confocal Microscopy works by illuminating the specimen with a laser. The laser light passes through a pinhole, then is reflected by the dichroic mirror and then focused by the objective lens on a small area of the specimen. The re-emitted light from the fluorophores has a longer wavelength than the laser, so it is then transmitted through mirror. It then passes through the pinhole where it is travel to the photo-detector.

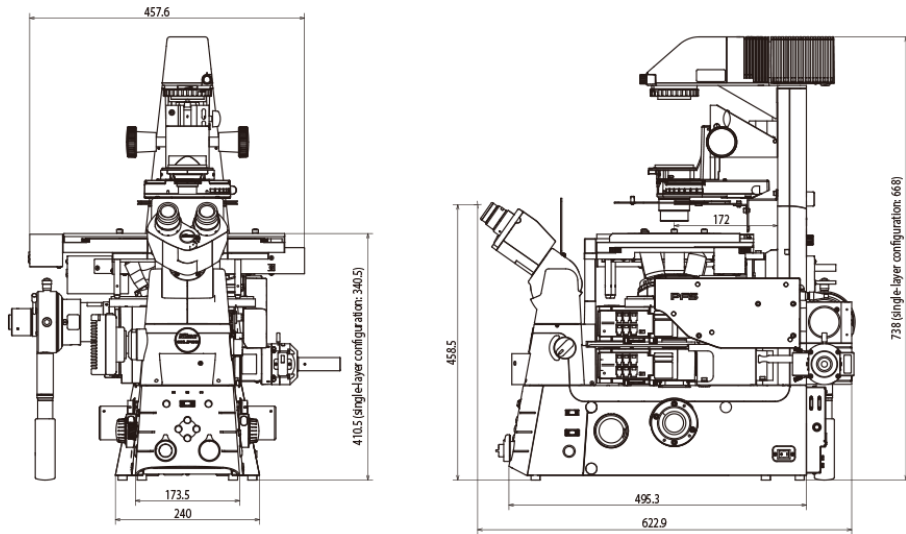


Figure 3.3: This may only be here because it's pretty....Also, I'd like to remove the measurements when I have time. Also, not sure how to cite the manual yet.

## 3.2 Applying Fluorescent Confocal Microscopy to our Sample

In order to see our substrate with fluorescent confocal microscopy, we need to coat the surface of our substrate with tiny fluorescent beads (fluorophores) on the order of 40nm in radius. The detection of these fluorescent beads allows us to see the outline of the substrate's surface, as well as the indenting sphere, which displaces the beads beneath it as it sinks into the substrate. Directions for preparing a fluorescent bead buffer can be found in Appendix section B.1.

### Fluorescent Confocal Microscopy Data Collection

Data was obtained using the Nikon A1R+ Confocal Microscope. To take image stacks of the Fluorescent beads, we use a 50x water-immersion objective lens. We set the laser to 440nm and adjust the power (HV) and gain as needed. Generally these values are around 5.0% and 40 Volts, respectively. In order to get clear locating, it is important not to saturate the photo-detector.

For silica spheres ranging from 5 – 50 $\mu\text{m}$  in size, we have found the best scaling factor to be .104 $\mu\text{m}/\text{pixel}$  in the horizontal plane for an image of 1024 x 1024 resolution. We set the vertical step size (z-direction) to .225 $\mu\text{m}/\text{px}$  or .25 $\mu\text{m}/\text{px}$  depending on what the confocal recommended. Both provided adequate vertical resolutions. 16x averaging using the resonant scanner took up to 5 minutes per scan, but provided excellent resolution.

### 3.2.1 Raw Data Files

Using confocal microscopy, we collect a “stack” of images, detecting the light from the fluorescent beads. Below (Fig. 3.4) is a raw data image of the surface of a soft substrate with a glass bead stuck below.

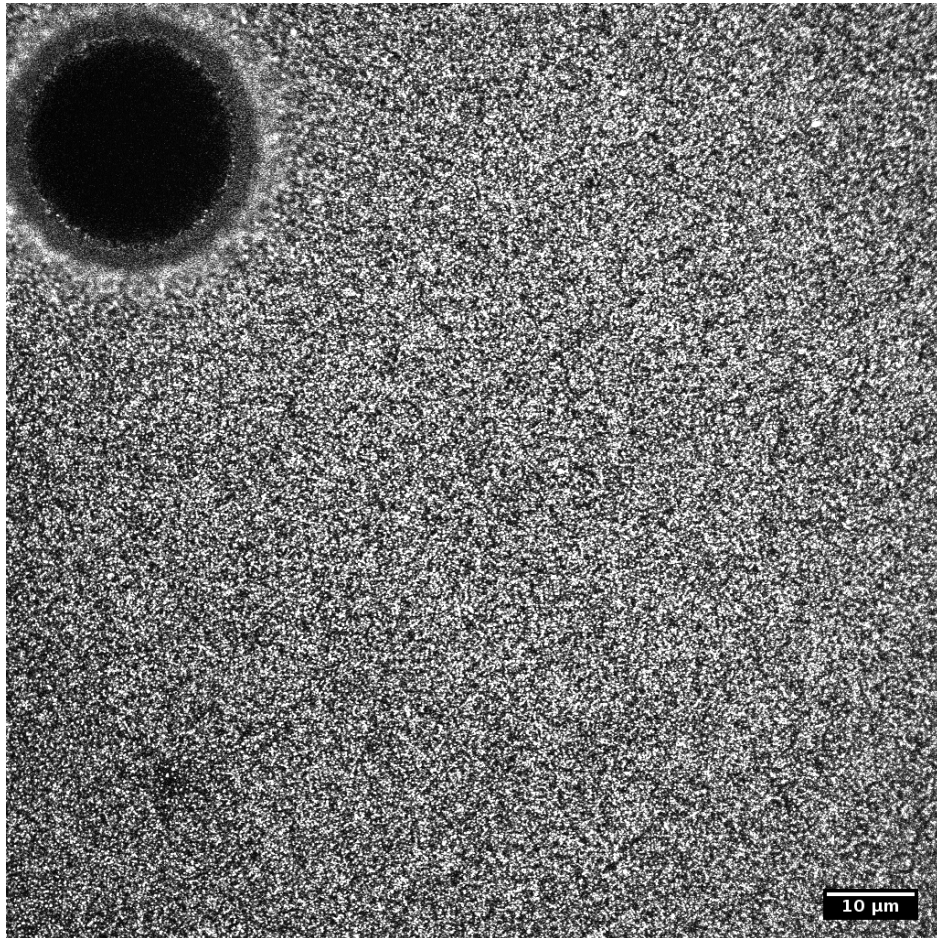


Figure 3.4: The surface plane of a silica bead in Gelest 9:1 Silicone ( $E = 7.3$  kPa). Radius of sphere =  $28.7\ \mu\text{m}$ .

The “black hole” like image in the top-left corner is the silica sphere. Each small white dot represents a fluorescent bead; together they create a sea of stars that outline the surface plane and the silica sphere. Figure 3.4 is an example of the upper limit of bead coverage density. Any higher concentration of fluorescent beads could result in a difficulty in light bleeding. Note, the sphere is in the top corner of the image to provide maximum information about the leveling of the surface plane. We assume that the surface effects are symmetrical for zero applied strain and equibiaxial strain. Thus, it is more important to gather information in one direction to properly level the surface plane to determine the depth into which the sphere sinks.

For each sphere, we take a stack of 50-100 images, depending on the size of the sphere. Figure 3.2.1 shows several vertical slices from the bottom of the sphere to just above the surface of the substrate.

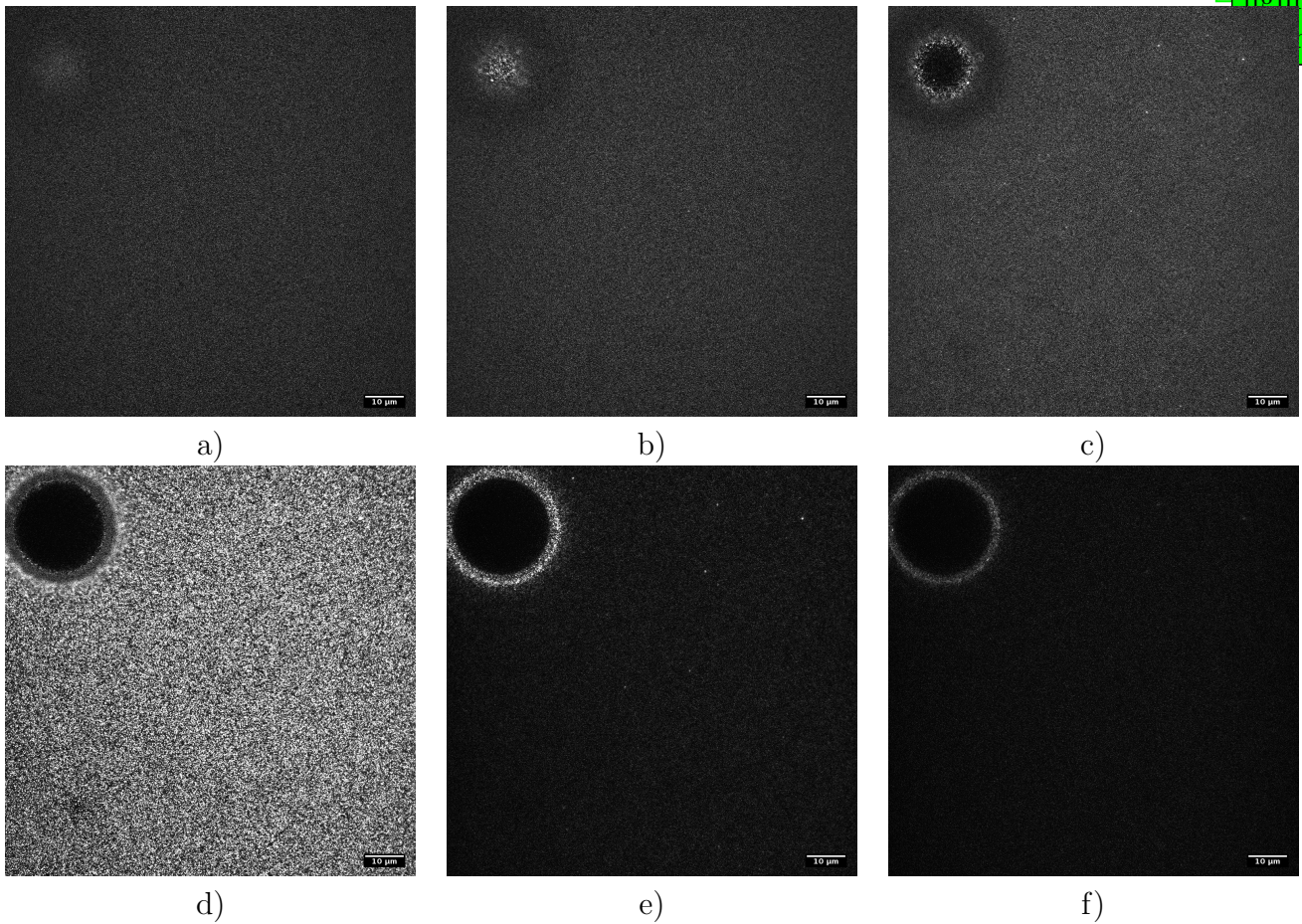


Figure 3.5: Images a-f display the x-y plane of the same sample traversing vertically from below the silica sphere to above the surface plane. The scale bar in the bottom right corners represent  $10 \mu\text{m}$

### 3.3 Image Analysis

In the following section, we will step through the process of analyzing a single sphere. Recall that in order to determine the surface stress and adhesion energy, we must fit equation 2.9 to the depth vs. radius measurements for a collection of spheres.

### 3.3.1 Particle Location

To turn a raw image file (saved as a .ome.tif) into usable data, we use a MATLAB program to locate each fluorescent bead. This is plotted in Figure 3.6. The flat orange plane of points is the surface, and the dark blue are the fluorescent beads pushed underneath the microsphere as it sinks into the substrate. It is easy to see the outline of the microsphere, and we can use this information to determine  $d$  and  $R$  for the sphere. Figure 3.7 shows the same sphere but stretched in the vertical axis to see the fluorescent bead density towards the bottom of the sphere.

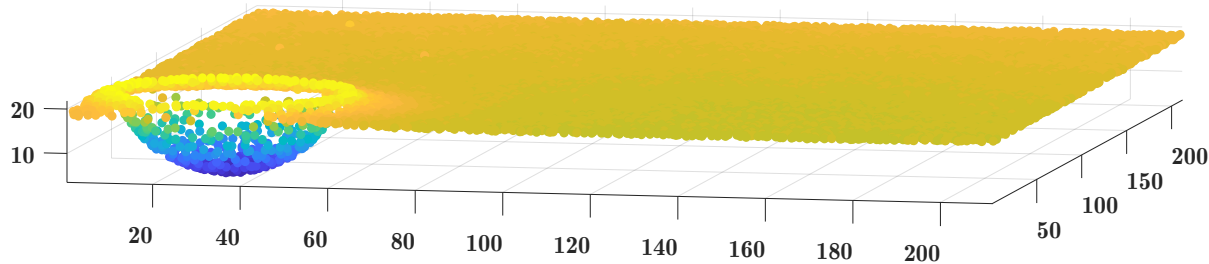


Figure 3.6: Using MATLAB software, we can locate each of the fluorescent beads in a given image stack. Here, we've plotted the located beads for the same sphere as in Figure 3.4 and 3.2.1. The dense blanket of orange points represents the surface of the substrate, and the blue points are the fluorescent beads pushed beneath the silica sphere during indentation.

### 3.3.2 Depth and Radius Determination

After locating all the fluorescent beads and reconstructing our raw image in a useful format, we can then use this information to extract the depth and the radius of the sphere. To accomplish this, we first determine the center of our sphere from the top (x-y plane) and collapse the side profile of the sphere. Figure 3.9 depicts the x-z plane as a cross-section through center of the sphere. We only need half of the sphere's profile to fit a circle. This ensures we have a large field of view to properly level and determine the substrate's surface. Figure 3.10 provides a zoomed in view of Fig. 3.9 to better indicate the resolution to which we try to fit a circle. Note the abrupt cut off around  $26 \mu\text{m}$  and how the substrate is lifted up above the zero-plane due to adhesion. Also notice the flatness of the substrate between  $26 - 29 \mu\text{m}$ . Not all samples have this flat ridge; many spheres lift the substrate to a point which then immediately slopes downward back to the zero-plane. This behavior depends slightly on the sphere size, but it is mainly a reflection of the amount of phase-separation induced. This is a property of the each silicone which depends on the environmental conditions.

It is important to be careful with the circle-fits in the case where the sphere is small enough to sink into the substrate with a depth  $d > r$ . In these instances, the side profile

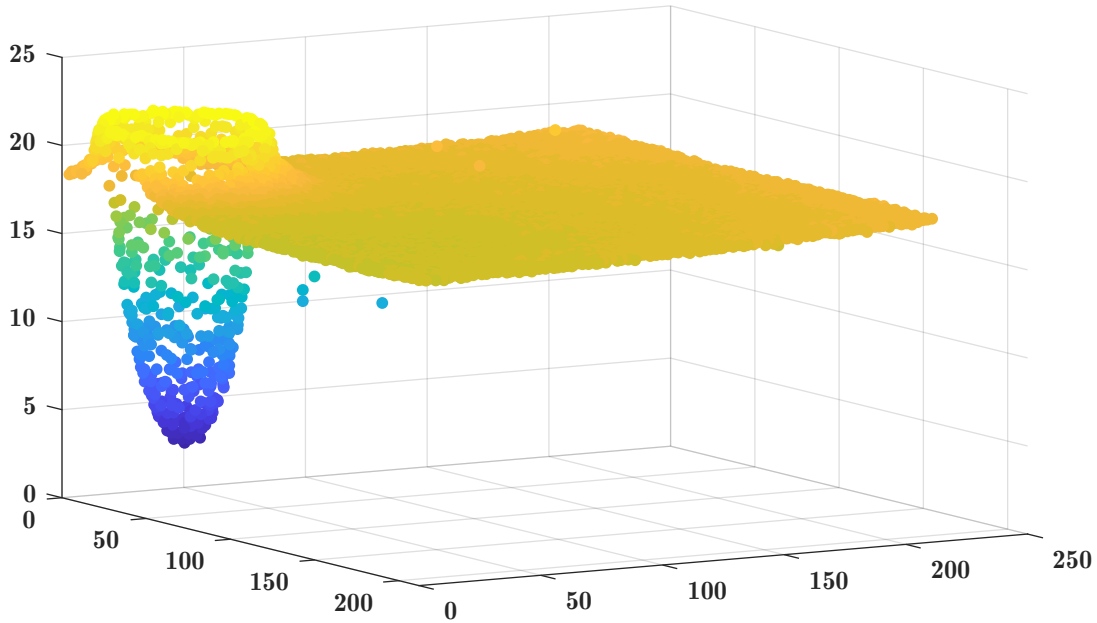


Figure 3.7: Fluorescent bead location for the same sphere as Fig. 3.6, only now it is stretched vertical axis to showcase the bead density under the bottom of the sphere.

is non-continuous, and we only fit the sphere to the bottom portion of the profile before the break.

Add an example profile of one of these tiny spheres

After fitting the circle to the substrate's side profile, we can add the depth vs the radius. The radius of the sphere is obviously just the radius of the circle, and the depth is the lowest point of the circle in the z-plane, which we center at  $x = 0$  in Figures 3.11 and 3.12.

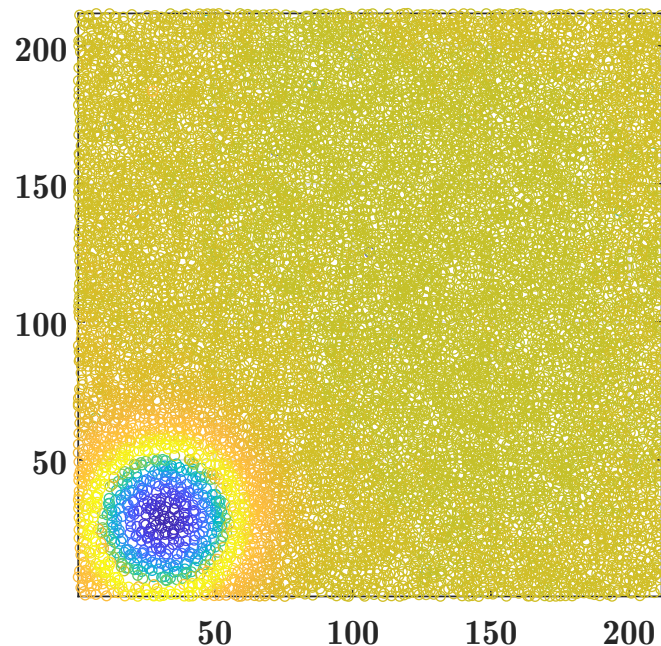


Figure 3.8: Here is the top view of the same sphere as in the previous figures. This allows us locate the center of the base of the sphere. From this we can construct a side profile (3.9)

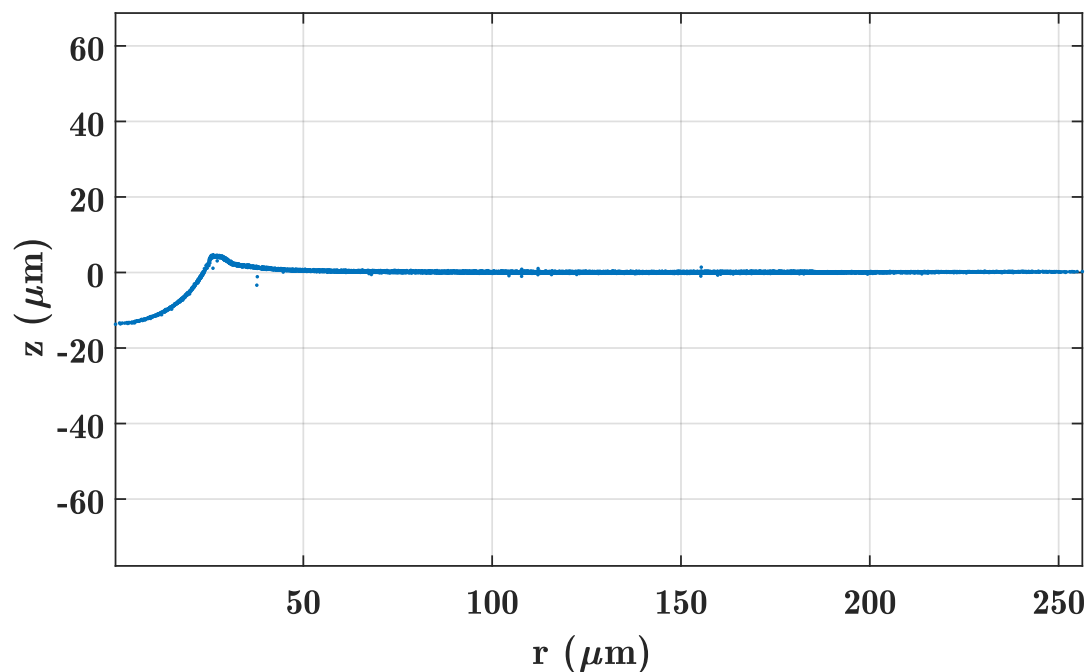


Figure 3.9: The constructed image of the outlined sphere with normalized axes. The Axes are in microns.

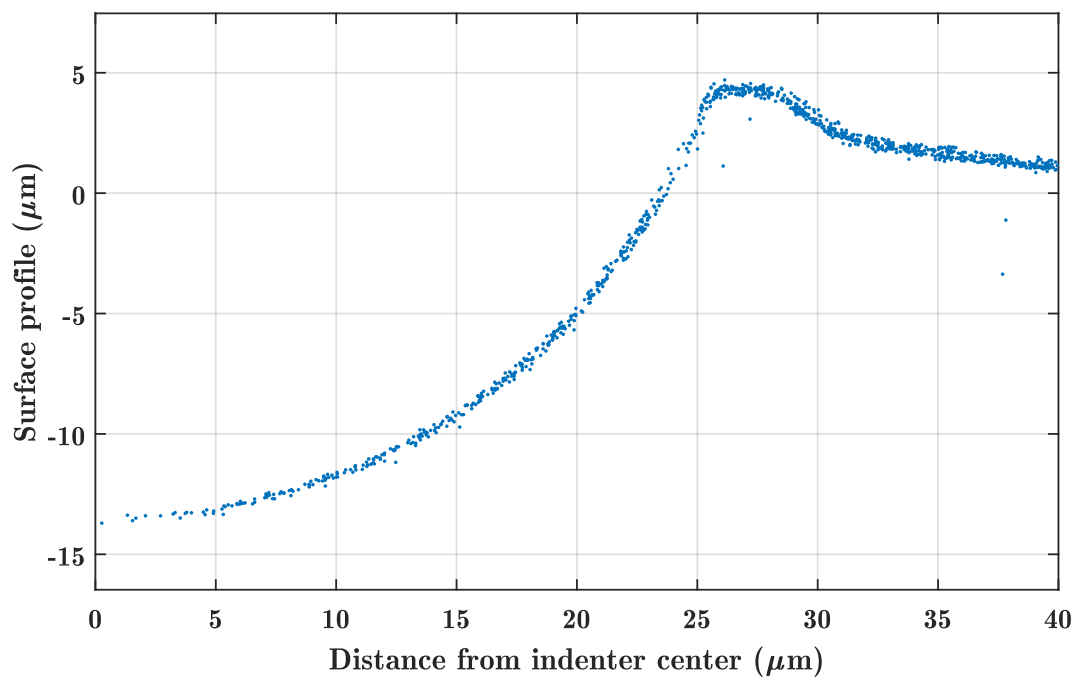


Figure 3.10: This is a zoomed-in version of figure 3.9. It is useful to zoom in and see the the quality of the collapse. A dense collapse leads to a smaller margin of error in fitting a circle to the profile (See Fig. 3.11).

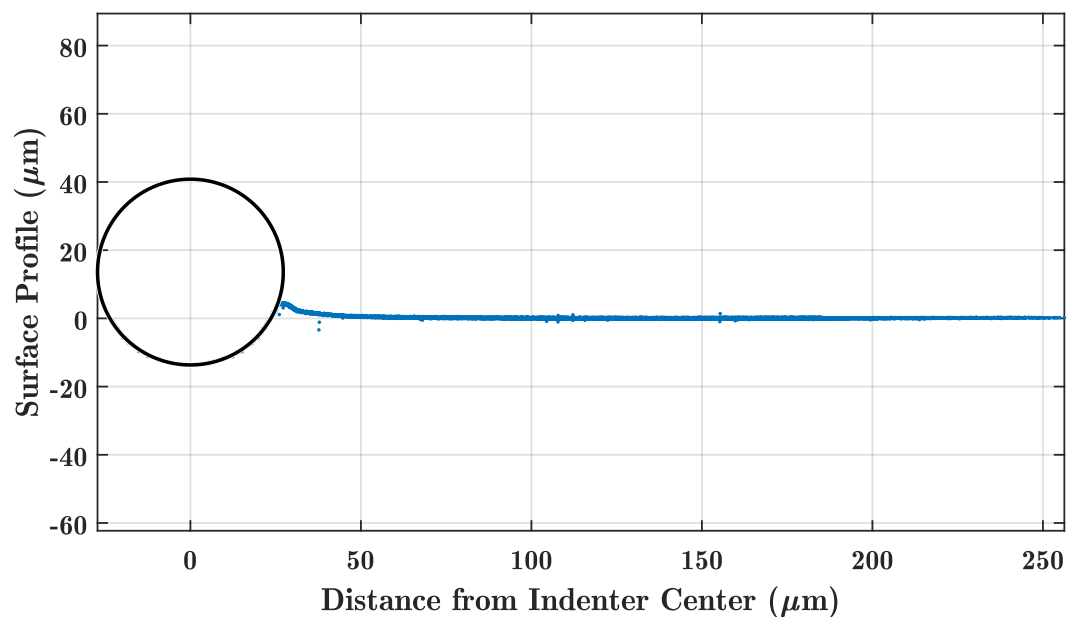


Figure 3.11: This is figure 3.9, only with a circle fitted to the indentation sphere. Notice how the surface plane is completely flat and centered at a depth of 0.

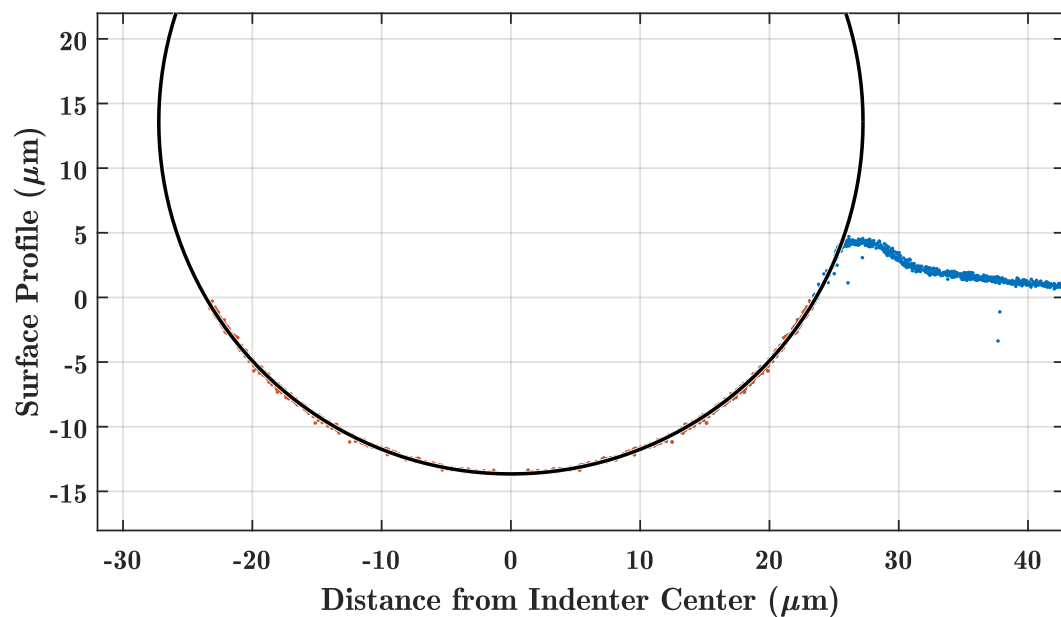


Figure 3.12: This is simply a zoomed in version of Fig. 3.11. The orange dots are the data points being used to fit the circle. Notice how the sphere fits nicely in the indentation all the way up to the cusp, past the points being used for the fit.

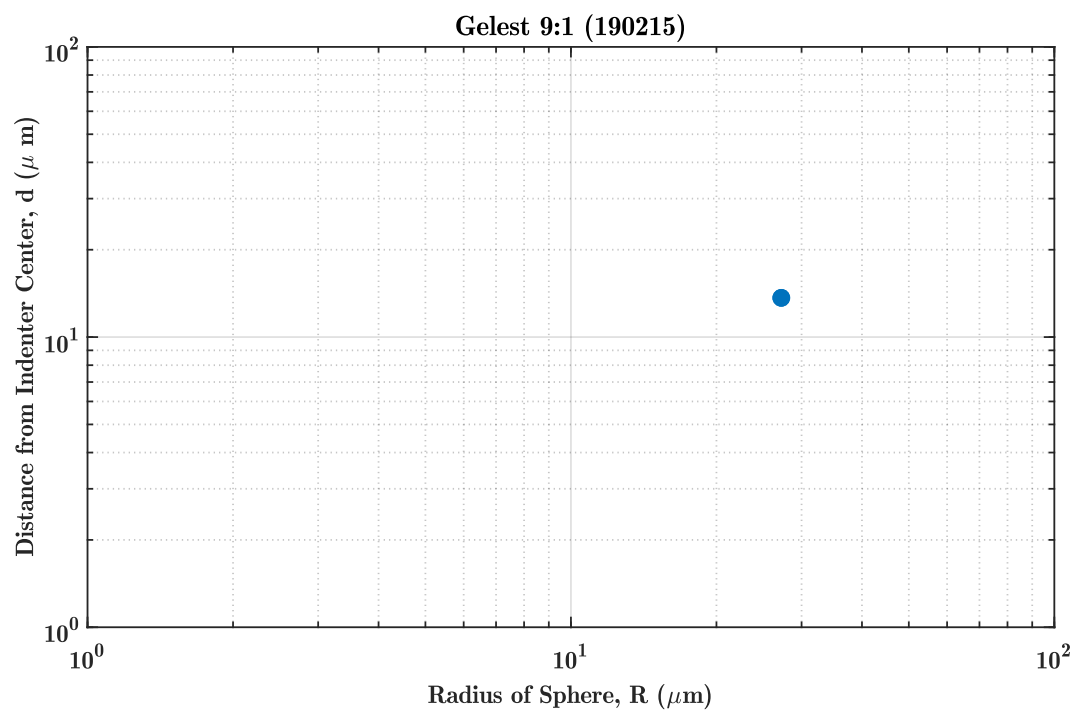


Figure 3.13: All of the above analysis leads to this single point, the depth,  $d$  vs. radius  $r$  for a given sphere. By repeating this process for many spheres of varying size, we can fill out the plot and fit 2.9 to the points. Examples of these fits can be found in Chapter 4.

# Chapter 4

## Surface Stress and Adhesion Results

In this chapter I present the surface stress and adhesion energy data collected for two types of silicone with various stiffnesses. We first used Gelest to obtain our preliminary data and tune the operation of our device. We then switched to Dow-Corning to continue more extensive measurements.

### 4.1 Organosilicon Polymer Chemistry

*MUST MOVE THIS. I should definitely talk about what the heck Silicone actually is, and what we're really using, and frankly why gels are stretchy. I think that I should say something in the introduction, and maybe designate an appendix if I want to go more in depth.*

PDMS, or Poly-Dimethyl-Siloxane, is a commonly used gel in the field of soft condensed matter. The gel is composed of a polymer network of crosslinkers, as well as a second polymer in the fluid phase. When stretched, the configuration of the system changes such that the tangled crosslinkers begin to unwind and untangle. From a statistical mechanics perspective, this decreases the configurational entropy, thus increasing the free energy. *Which free energy though? I think this is what we're covering next in 302...Also I got this from that unpublished review article*

Below (Fig. 4.1) is the chemical structure for the vinyl-terminated PDMS (Gelest) that comprises the fluid phase.

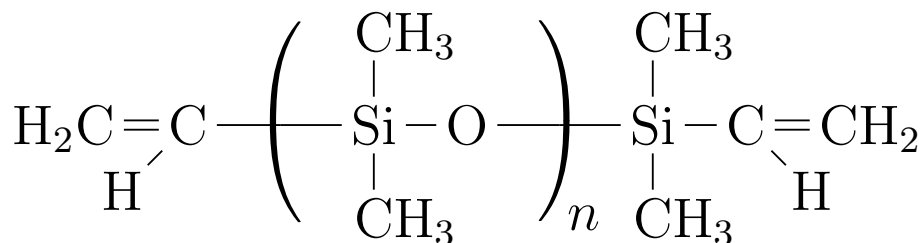


Figure 4.1: Divinyl-terminated Polydimethylsiloxane (DMS-V31)

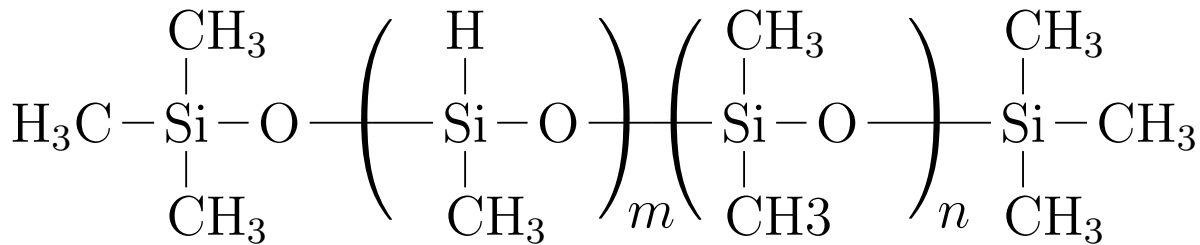


Figure 4.2: Trimethylsiloxane terminated 25-35% methylhydrosiloxane ( $m$ ) - dimethylsiloxane ( $n$ ). This is the crosslinker. *I could make that lone H red to help make clearer where the crosslinker bonding is happening. Thoughts?*

The crosslinker for the system is a trimethylsiloxane terminated 25-35% methylhydrosiloxane - dimethylsiloxane copolymer. The crosslinker is much shorter on average than the PDMS, containing roughly 20-30 repeating monomer groups. The single hydrogen on the methylhydrosiloxane is weakly bound, and can be replaced by one of the hydrogen atoms in the PDMS. This bonding happens over and over again, creating the long twisted chains that create the mesh network of the gel. Increasing density of crosslinkers provides an easy and controllable method to vary the gel's stiffness.

Table 4.1: PDMS gel characterization

Mix Ratio (A&B)	Young's Modulus (kPa)	Sol Fraction (%)
7.5 : 1	2.5 $\pm$ 0.1	65.2
9 : 1	5.0 $\pm$ 0.1	64.7
11 : 1	10.0 $\pm$ 1	63.7

## Overly Specific Silcone Preparation and Spin Coating

This whole section needs to be fixed. It's a detailed version of the outline in ch. 2

*this probably sounds unclear. Change Later.* We know the stiffness of the gel we are curing, and by having a thick enough coating, we can ensure that the microspheres are only interacting with this gel.  $100 \mu\text{m}$  is a reasonable aim, and our substrates generally are between  $80 - 100 \mu\text{m}$ . The second concern is with thickness. In principal, as long as the surface is locally flat with respect to each microsphere, we can determine where the surface level lies and still measure the depth. In reality, it is not difficult to produce an even coating of silicone using a spin-coater.

Before spin-coating it is useful to coat the underlayer with fluorescent beads. It is not vital, but this is helpful in determining the substrate's thickness. The only information obtained by this coating is the location of the substrate's bottom surface, so a dense bead coverage is not required, and could potentially be harmful if there is light bleeding. I suggest

coating the bottom surface with 40nm beads for 1 minute. Full directions for preparing a fluroescent bead solution can be found in Appendix B. After this time, you may return the fluorescent beads back to the solution for re-use. A significant number of beads will remain on the underlayer. To remove some excess, gently wash the substrate with de-ionized water. For a coverslip, simply submerge the entire slip in water and gently remove it at a 45°angle, trying to prevent the water from breaking-up into smaller droplets. This process is slightly more difficult for the petri dish due to the larger size. I suggest (either) using a very large container of water (it can be shallow, really you just need a large opening). If this proves challenging, I have found success using a 1000mL beaker tilted at an angle. It is also possible to use an autopipet for washing; repeat the same process used for the fluorescent bead coating, only use water this time. I have had mixed success with this technique, however. It often leaves a water droplet and has led to an uneven coating of fluorescent beads, manifested as streaks across the surface.

Depending on the silicone, a different amount of time should be waited before spin coating onto the desired surface. We coat our substrate onto glass for "zero applied strain" data or onto PDMS *yeah I gotta look up the brand when I get back. I totally forget.* for stretching data. It is best that the silicone is far enough along in the curing process that it has enough stiffness and cohesiveness to remain on the underlayer when spun. As an extreme example, consider trying to spin-coat water; it would all fling off the underlayer. *is there a better term than underlayer. I'm thinking of the general term for what we use a coverslip or stretchy circle.* For Gelest 9:1, there is no waiting time necessary; Gelest 9:1 cures rapidly. For Dow Corning 1:1, a wait time before spinning of 1 hour was observed.

To help with the evenness of the coating, it is useful to degas the gel by leaving it in a vacuum chamber for a few minutes. A few small bubbles are not of concern, as the process of transferring the gel to the underlayer is enough to pop any remaining stragglers. I have found that a "glob" of gel roughly half the diameter of the underlayer, with the spin-coater set to 500rpm for 40sec is enough to create an even coating of roughly 100  $\mu\text{m}$ .

Coating a coverslip with silicone is a straightforward process where hardly anything can go wrong. Coating the stretchable PDMS underlayer, however, requires some creativity to find the steps necessary to return the best results. I cut the PDMS disk with an X-acto knife and using a standard Petri *2.5in diameter ...look up* dish as a template. In order to avoid snagging, I suggest cutting out the circle before removing the paper sheets on both sides of the silicone. Taping the Petri dish to the paper is also helpful prevent the dish from slipping while cutting. Unlike the glass coverslip, the PDMS underlayer is not rigid and must be place on a ridgid surface, such as a Petri dish, for spin coating. This leave the possibility that air bubbles could be trapped in between the PDMS and the Petri dish. This is a surefire way to ensure an uneven and frustrating substrate. I suggest removing the top paper sheet of the newly cut PDMS, then placing the Petri dish down upon the exposed silicone. You should now have a Petri dish with a silicone disk on top and a paper sheet on top of that. Using your thumbs, simply do your best to push all the air bubbles from the center outwards. Finally, any tiny air bubbles can hopefully be removed by placing the Petri dish in a vacuum chamber for a few minutes. Now you can coat the PDMS with fluorescent

beads and wash as desired before place the petri dish onto the spin-coater and proceeding as described above.

After spin-coating, the silicone requires time to cure. We cure Dow-Corning 1:1 for at room temperature for at least 24 hours. For Gelest 9:1, we oven cure at 70° C for at least 24 hours. Either silicone can be cured at room temperature or in the oven so long as a sufficient amount of time is waited, however, we have used this methods to maintain consistency, as well as parallel the techniques used in previous literature [1].

After the silicone cures, it is time to coat the surface with fluorescent beads again. It is important that the beads are dense enough to give a high resolution, yet not so dense as to become indistinguishable; this presents a challenge the MATLAB particle locating software. Secondly, too dense a bead coverage risks light bleeding to vertically adjacent stacks. For the 40nm bead solution prescribed in Appendix B, I suggest letting the solution soak for up to 3 minutes before removing and washing the substrate. While the fluorescent beads chosen are most susceptible to light at *shoot, what wavelength? Like 440?* nm, there is still the risk of photobleaching the fluorophores, and worth dimming the lights in the lab when working with them.

## 4.2 Preliminary Data: Gelest

Because Figure 1 was obtained using Dow-Corning silicone gel, our intention from the start was to use this material in our adhesion based measurements. Because the material was back-ordered, we used Gelest instead while we calibrated the process. I present this preliminary data because it shows clear incremental steps of evidence that the surface stress for the substrate is increasing under strain.

### 4.2.1 Standard Candles

Not only do we measure the depth and radii for a range of spheres, but we also measure a select few spheres at every strain. This allows us to track how any given sphere is changing, increasing our confidence that the shift in  $\Upsilon$  and  $W$  is not just an artifact of noise. Below is the side profile for Gelest 9:1 ( $E = 6.3$  kPa). Notice how the profile shifts noticeably upwards to be flattened when the substrate is stretched. This shift is expected if the surface stress is increasing (see equation 2.9).

## 4.3 Dow-Corning PDMS

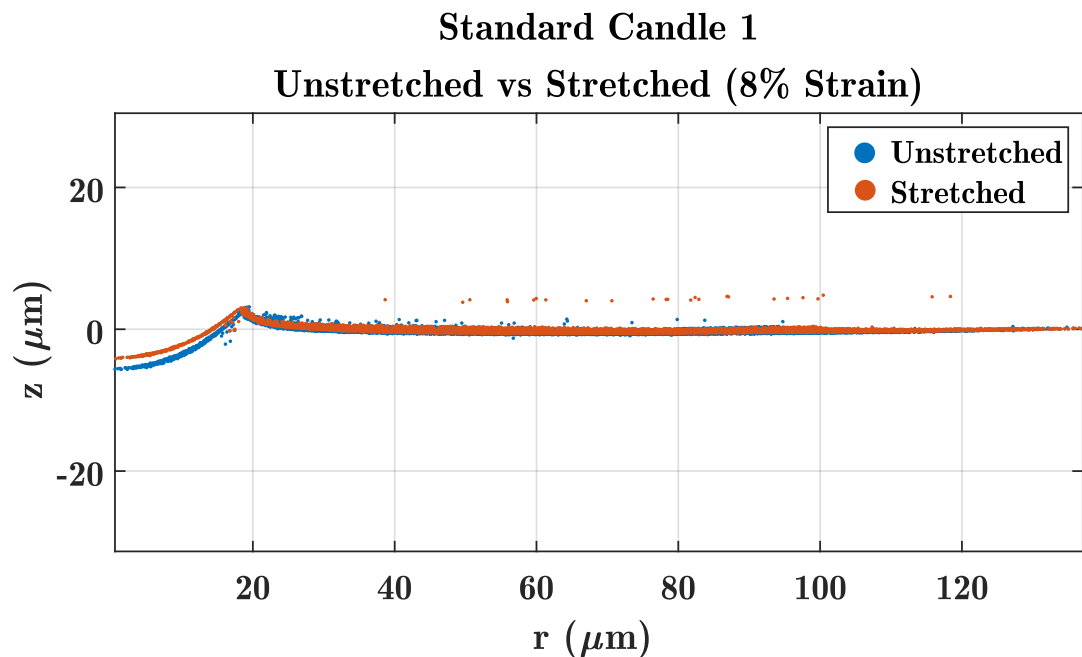


Figure 4.3: The side profile of the same sphere before and after stretch. Notice how after stretching, the sphere's indentation into the substrate is shallower. Substrate is Gelest 9:1 ( $E = 6.3$  kPa).

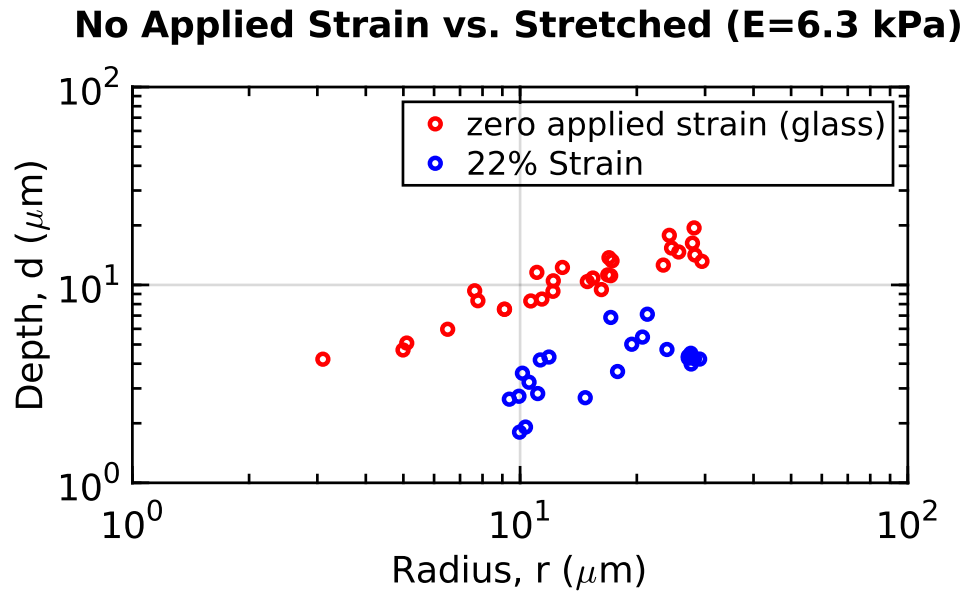


Figure 4.4: For Gelest 9:1. The silicone under strain (blue) on average sink less deep into the silicone than the same silicone spun on glass (zero applied strain) *COME BACK TO THIS AND FIX THE PLOT TO MAKE IT MATCH THE OTHERS*

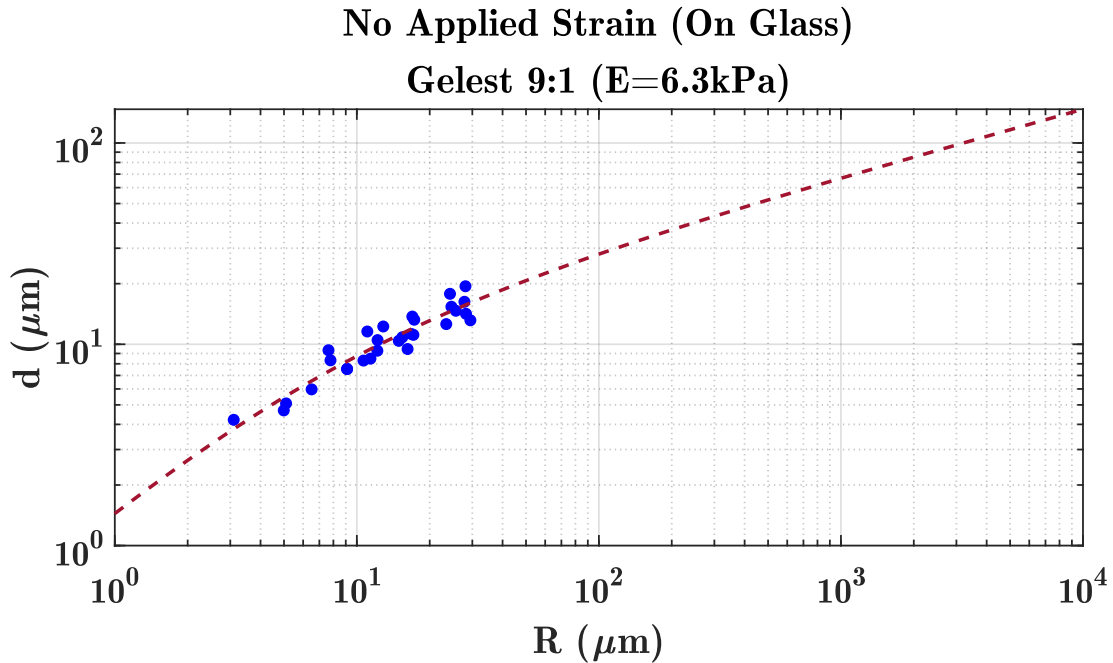


Figure 4.5:

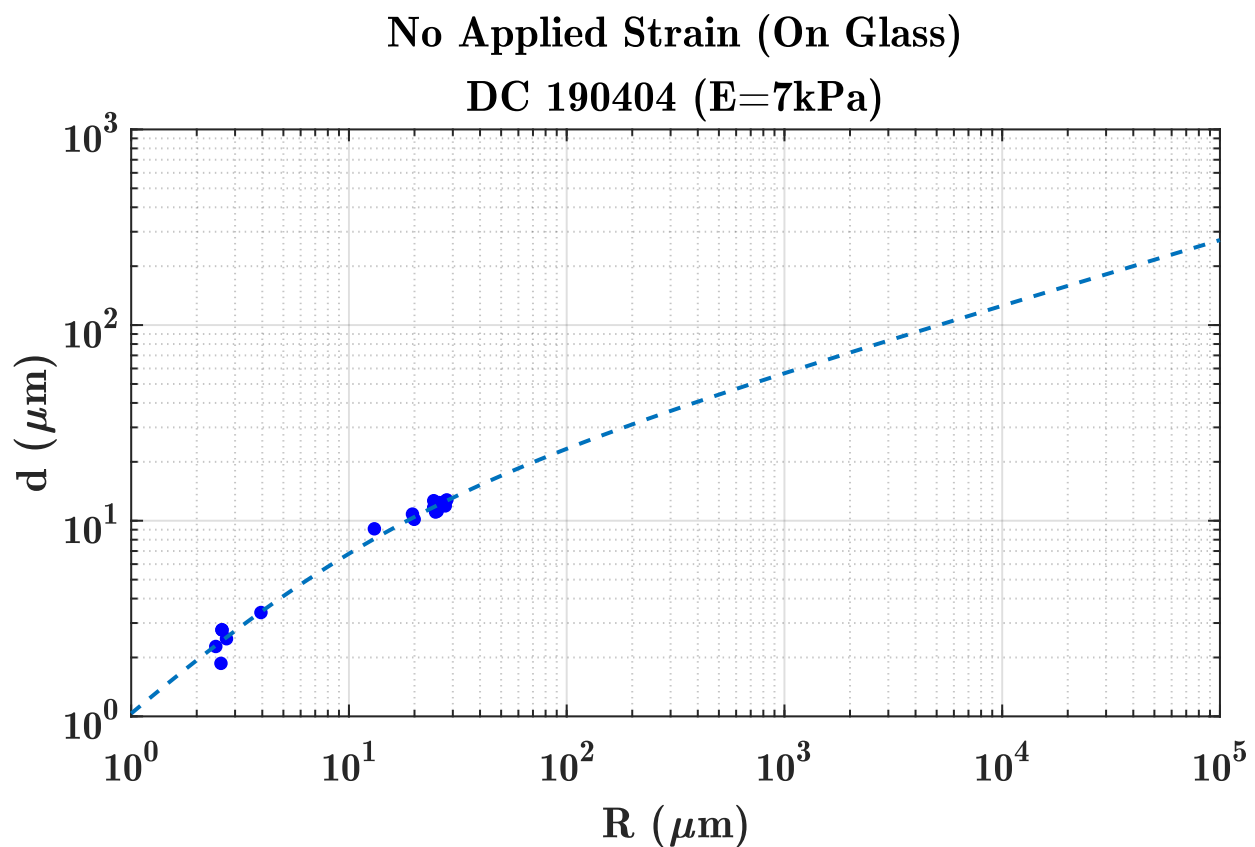


Figure 4.6: The surface stress and adhesion energy fit for Dow Corning PDMS silicone with no applied strain. Given the  $d$  vs.  $R$  values, the fitting parameters to make the best fit line are  $W = 48.6$  and  $\Upsilon = 43.5 \text{ mNm}^{-1}$ .

# Chapter 5

## Future Work

*I still feel like pushing things off and saying, “oh I’ll get to this before my thesis is due,” yet deadlines are approaching and I guess I need to face reality.* As boasted, the adhesion based technique for measuring  $\Upsilon(\epsilon)$  should be applicable to any soft solid capable of being stretched. Naturally, we would like to expand our measurements beyond silicone. Hydrogels, aerogels, and gelatins, to name a few, are objects of interest. Commercial adhesives are a subject of financial interest, with possible consequential technological developments.

### 5.1 Neue Materialen: Gummibärli

Measuring the strain dependent surface stress of a gummy bear presents challenges not present in PDMS silicone. For example, gummy bears come in a predefined size and shape. In order to spin coat them on our apparatus, we must first melt down the gummies. Gummy bears are composed primarily of gelatin and a glucose syrup. When melted, *I should chat with adam about what’s happening to continue this section.*

# Appendix A

## Stretching Apparatus Engineering Design Document

### A.1 Details of Stretcher Design

Moved to Appendix. Revise writing.

Aluminum was chosen as the base material because of its sturdy yet malleable nature, making it an excellent material with which to mill. Acrylic was considered, but was not chosen because of its brittle nature; we were concerned about cracking when drilling the UNF threads connecting to the Luer-lock syringe.

The stretched sheet is laid over the lubricated apparatus and fixed in place using a 48.7mm diameter by 1.6mm thick rubber O-ring. A removable plastic ring is then placed on top of the o-ring and clamped down using a tension clamp attached to a fitted plastic base slotted for the stretching apparatus to sit. The plastic ring is constructed from an engineering plastic that came from a similar but malfunctioning device used by our colleagues at ETH Zürich. The outer ring could easily be laser cut from a plastic or milled out of aluminum if desired.

To pull a vacuum, a 1/4-28 UNF to female Luer connects the apparatus to a plastic 100ml Luer-lock syringe. We found a more consistent stretch was held by lining the inner walls of the syringe in more Dow Corning vacuum grease. The UNF to female luer connector is stainless steel, and *sealed into place with epoxy resin. Note: I haven't done this yet 190322, but I think I should. But make sure to get the o-ring size first...and i think one size smaller would actually work better* coated with Dow Corning vacuum grease. The inclusion of a small o-ring between the UNF threads and the cylindrical base proved critical in holding vacuum for sustained periods of time.

The vacuum pull was controlled by a Harvard Apparatus Elite 11 Syringe Pump. This allows us to have a consistent withdraw rate and control over the amount of air withdrawn down to the pico-liter level, a far greater precision than needed. Stretching was found to work best at maximum withdrawal rate. Our stretching apparatus has sustained a constant

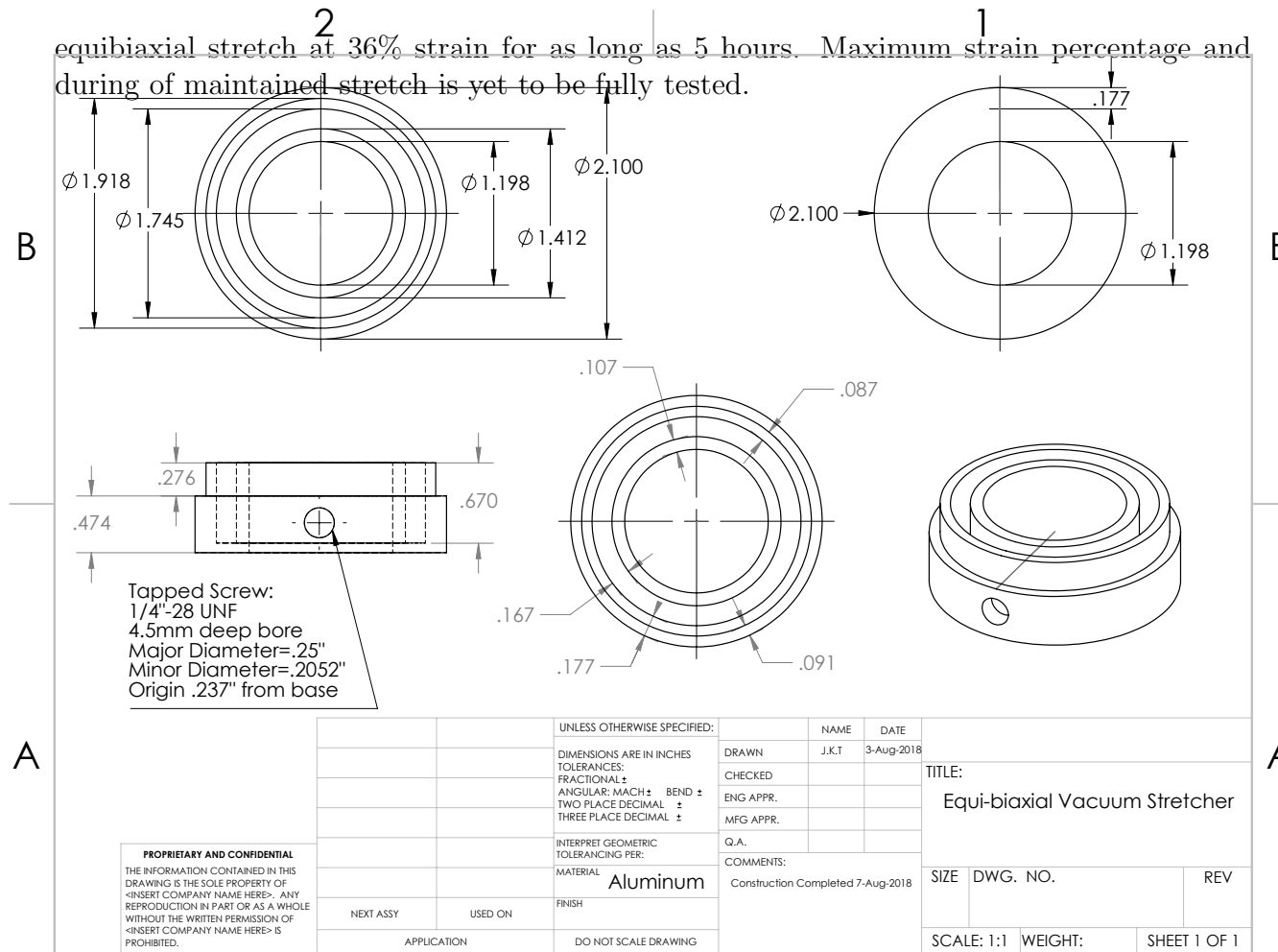


Figure A.1: The equi-biaxial vacuum stretcher design document. Note: all measurements are in inches.

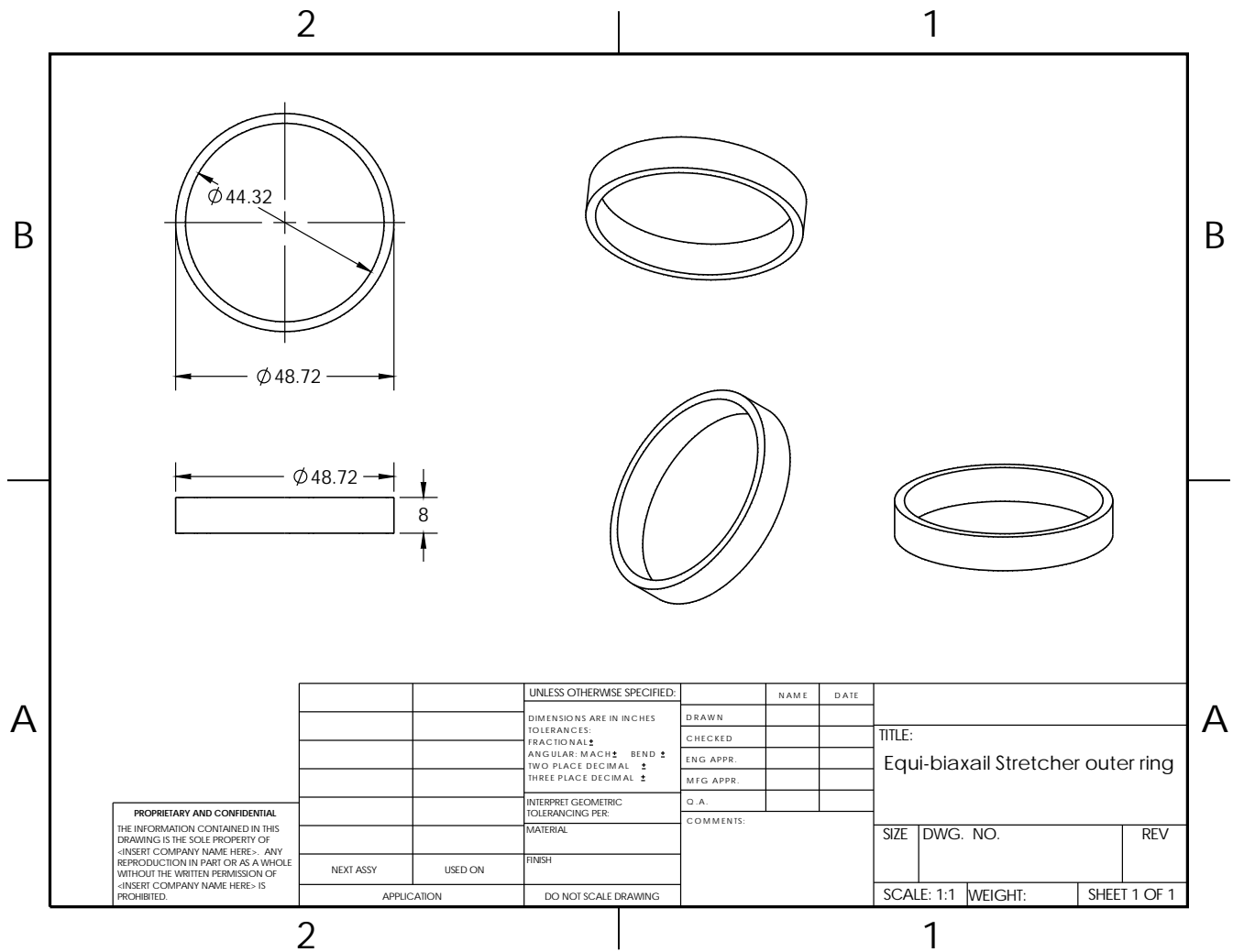


Figure A.2: Engineering Design Document of the outer-ring for the Stretching Apparatus.  
Note: all measurements are in millimeters. (UGH, why is the base in imperial and the ring in metric?! Must fix this - Jeremy )

# Appendix B

## Fluorescent Bead Recipe

### B.1 Preparing a Fluorescent Bead Solution

Ok, the recipe is in my lab notebook in lab. IT won't take me long to write this appendix. Here's what to include

- Directions and Recipe with the borate buffer solution - Make sure to also note that the solution should be wrapped to avoid light exposure and to keep them in the refrigerator.

# Appendix C

## MATLAB Code

Looking at previous majumder theses, they all seem to include appendices with their matlab code. I think I have too much to include the actual code, but I think it would be useful to include what .m files I use, what they do, and in what order to run them. How else will someone know what to do with them? I also think it would be useful to put them in my github account in a new project folder and permilink there.

### C.0.1 Confocal Analysis Codes

Below I list the MATLAB codes used in analyzing the raw .ome.tif files obtained from the confocal imaging process. I will list them in the order executed to obtain the desired d vs. R values. In each description, I will also include the required files needed to run the script.

#### `iterative_locating_input_parameters_2018.m`

- Set particle locating parameters such as estimated particle size, brightness intensity range, and minimum separation
- Define the image stack to be analyzed
- Rescale the image from pixels to microns

#### `iterative_particle_locating.m`

- Locates the fluorescent beads
- Returns a .txt file with the locating information and creates a figure
- INCLUDE FIGURE HERE

**process\_and\_collapse\_confocal\_data.m**

- Estimate the center point of the sphere in the format of `[x,y]` + `return`
- Follow the directions printed on the screen to collapse the side profile of the sphere
- INSERT SIDE PROFILE. CAPTION: A PROPERLY COLLAPSE SIDE PROFILE LOOKS AS FOLLOWS

**circle\_fit\_confocal\_profiles.m**

- You must edit this script for the first time you analyze a sphere for a given data set.
- This script fits a circle to the collapsed side profile
- Script saves the  $d$  vs  $r$  value as a .mat file, adds the `[d,r]` data to a list of all `[d,r]` values (or creates that list if it's the first time being run for a data set), and plots the  $d$  vs.  $r$  data

### C.0.2 Strain Calculation Codes

The codes used for calculating the strain are credited to Rob Styles (I think. I need to check who wrote what).

**master\_tracking\_gui.m**

### C.0.3 Silicone Characterization Measurements

To measure the stiffness of our silicone (Young's Modulus, E), we use the *something something Texture Analyzer*. We measure the force of resistance (N) vs. depth of compression (m) for several points near the center of the bulk. We only use points near the center to isolate the silicone. Measuring near the sides could include the restorative force from the walls of the container.

**measure\_modulus.m**

- Calculates the average slope of this curve. This is the Young's Modulus of the substrate.  $(\sigma/\epsilon)$
- The requested starting position is the x-axis value where the linear slope approximately begins. It is better to overshoot the starting value than undershoot it

# Bibliography

- [1] Q. Xu, K. E. Jensen, R. Boltyanskiy, R. Sarfati, R. W. Style, and E. R. Dufresne. *Direct measurement of strain-dependent solid surface stress*. Nature communications, 8(1):555 (2017).
- [2] R. C. Cammarata and K. Sieradzki. *Surface and interface stresses*. Annual Review of Materials Science, 24(1):215–234 (1994).
- [3] J. W. Gibbs. *The scientific papers of J. Willard Gibbs*, volume 1. Longmans, Green and Company (1906).
- [4] P.-G. d. Gennes. *Capillarity and wetting phenomena : drops, bubbles, pearls, waves*. Springer, New York (2003).
- [5] C. Mays, J. Vermaak, and D. Kuhlmann-Wilsdorf. *On surface stress and surface tension: II. determination of the surface stress of gold*. Surface science, 12(2):134–140 (1968).
- [6] H. Wasserman and J. Vermaak. *On the determination of a lattice contraction in very small silver particles*. Surface Science, 22(1):164–172 (1970).
- [7] R. Hanneman, M. Finn, and H. Gatos. *Elastic strain energy associated with the “a” surfaces of the iii–v compounds*. Journal of Physics and Chemistry of Solids, 23(11):1553–1556 (1962).
- [8] R. E. Martinez, W. M. Augustyniak, and J. A. Golovchenko. *Direct measurement of crystal surface stress*. Physical review letters, 64(9):1035 (1990).
- [9] A. Schell-Sorokin and R. Tromp. *Mechanical stresses in (sub) monolayer epitaxial films*. Physical review letters, 64(9):1039 (1990).
- [10] R. W. Style et al. *Stiffening solids with liquid inclusions*. Nature Physics, 11(1):82 (2015).
- [11] E. R. Jerison, Y. Xu, L. A. Wilen, and E. R. Dufresne. *Deformation of an elastic substrate by a three-phase contact line*. Physical review letters, 106(18):186103 (2011).
- [12] M. E. Gurtin and A. I. Murdoch. *Surface stress in solids*. International Journal of Solids and Structures, 14(6):431 – 440 (1978).

- [13] R. W. Style, R. Boltyanskiy, Y. Che, J. Wetlaufer, L. A. Wilen, and E. R. Dufresne. *Universal deformation of soft substrates near a contact line and the direct measurement of solid surface stresses.* Physical review letters, 110(6):066103 (2013).
- [14] X. Xu, A. Jagota, D. Paretkar, and C.-Y. Hui. *Surface tension measurement from the indentation of clamped thin films.* Soft Matter, 12(23):5121–5126 (2016).
- [15] K. E. Jensen et al. *Wetting and phase separation in soft adhesion.* Proceedings of the National Academy of Sciences, 112(47):14490–14494 (2015).
- [16] S. Mondal, M. Phukan, and A. Ghatak. *Estimation of solid–liquid interfacial tension using curved surface of a soft solid.* Proceedings of the National Academy of Sciences, 112(41):12563–12568 (2015).
- [17] A. Jagota, D. Paretkar, and A. Ghatak. *Surface-tension-induced flattening of a nearly plane elastic solid.* Physical Review E, 85(5):051602 (2012).
- [18] N. Nadermann, C.-Y. Hui, and A. Jagota. *Solid surface tension measured by a liquid drop under a solid film.* Proceedings of the National Academy of Sciences, 110(26):10541–10545 (2013).
- [19] S. J. Park, B. M. Weon, J. San Lee, J. Lee, J. Kim, and J. H. Je. *Visualization of asymmetric wetting ridges on soft solids with x-ray microscopy.* Nature communications, 5:4369 (2014).
- [20] K. L. Johnson, K. Kendall, and A. Roberts. *Surface energy and the contact of elastic solids.* Proc. R. Soc. Lond. A, 324(1558):301–313 (1971).
- [21] H. R. Hertz. *Über die berührung fester elastischer korper.* Verhandlung des Vereins zur Beförderung des Gewerbelebens, Berlin, p. 449 (1882).
- [22] R. W. Style, C. Hyland, R. Boltyanskiy, J. S. Wetlaufer, and E. R. Dufresne. *Surface tension and contact with soft elastic solids.* Nature communications, 4:2728 (2013).
- [23] Z. Cao and A. V. Dobrynin. *Nanoparticles as adhesives for soft polymeric materials.* Macromolecules, 49(9):3586–3592 (2016).
- [24] S. Na, A. Trache, J. Trzeciakowski, Z. Sun, G. Meininger, and J. Humphrey. *Time-dependent changes in smooth muscle cell stiffness and focal adhesion area in response to cyclic equibiaxial stretch.* Annals of biomedical engineering, 36(3):369–380 (2008).
- [25] M. Marvin. *Microscopy apparatus* (1961).